Transport properties of modified concrete by surface and bulk hydrophobization via nano-clay addition

Maria Letizia Fariello

Unione Europea

Ministero dell'Istruzione, dell'Università e della Ricerca

UNIVERSITÀ DEGLI STUDI DI SALERNO

Department of Chemical and Food Engineering

Ph.D. Course in Chemical Engineering
(X Cycle-New Series)

TRANSPORT PROPERTIES OF MODIFIED CONCRETE BY SURFACE AND BULK HYDROPHOBIZATION VIA NANO-CLAY ADDITION

Supervisor
Prof. Luciano Di Maio
Prof. Loredana Incarnato

Ph.D. student
Ing. Maria Letizia Fariello

Scientific Referees
Prof. Domenico Caputo
Prof. Luc Courard

Ph.D. Course Coordinator
Prof. Paolo Ciambelli

To my family

Acknowledgments

This PhD work was made possible by the support and assistance of a number of people whom I would like to personally thank.

I would like to express my gratitude to my supervisors, Prof. Luciano Di Maio and Prof. Loredana Incarnato, whose expertise, understanding, and patience, added considerably to my graduate experience. Thanks to them, throughout these three years of PhD course, I had many opportunities of scientific interactions (congresses, seminars, workshops), which often resulted in ideas and suggestions.

Not less important, during the last year, I had the opportunity to spent six months at the University of Liège, in Belgium, to deepen some thematic aspects of my research project. Here I worked under the supervision of Prof. Luc Courard, who, with his team-work, gave me a very warm welcome. I would like to thank each of them for the time they dedicated to me. This wonderful period I spent abroad has been for me a very important occasion for personal enrichment, not only from the scientific point of view but also human, beyond the fact that I had the opportunity to visit a very amazing Country.

This Thesis owes a lot to Prof. Paola Scarfato, for her help in interpretation of the experimental results and invaluable advices to this work.

I am very grateful to Prof. Paola Russo for her important contribution in the Porosimetry analyses.

A special "thank you" goes to Dr. Ing. Francesco Marra for supporting me in modeling the chloride diffusion results.

A big thanks to my colleagues and friends Dr. Elvira Avallone, Dr. Ing. Maria Rosaria Galdi and Dr. Ing Emilia Garofalo for the pleasant moments spent together and the conversations shared daily

during the lunch time or the coffee breaks. Even if unconsciously they gave me the motivation and the charge also in the difficult moments.

I would like to thank Salvatore Montesano for his very helpful contribution, in the initial part of my work, to the preparation of concrete samples, difficult task for a woman.

An obligatory thanks goes to my family, especially to my parents. They gave more than I deserve and they never denied me the encouragement and the support during the months away from Italy. Thank also to my brother because even if far, he is always and constantly worried about me and about everything I do.

I want to thank also my boyfriend, for the love he demonstrated me supporting all my choices and for being my valve vent in the most critical moments.

Finally I would like to thank everyone who made me feel their closeness in these years and that it's not possible mention here one by one.

List of publications

National and International Congresses:

L. DI MAIO, **M. L. FARIELLO**, P. SCARFATO, L. INCARNATO, L. COURARD, F. MICHEL, Transport properties of nano-clay modified hydrophobic concrete. 2nd workshop on The new boundaries of structural concrete, ACI Italy Chapter, Università Politecnica delle Marche, Ancona, 15 - 16 settembre 2011. ISBN 978-88-904292-2-4

L. DI MAIO, **M.L. FARIELLO**, P. SCARFATO, L. INCARNATO. Water absorption and gas transport properties of a hydrophobic nanocomposite concrete. VIII Convegno Nazionale sulla scienza e tecnologia dei materiali - INSTM. Grand Hotel Baia Verde – Aci Castello (CT), 26-29 Giugno 2011. p: P31.

P. SCARFATO, **M.L. FARIELLO**, L. DI MAIO, L. INCARNATO. Trattamenti superficiali per la protezione del calcestruzzo mediante l'utilizzo di resine nano composite. Atti del 10° Convegno nazionale AIMAT. Capo Vaticano, 5-8 Settembre 2010. pp: 569-572, ISBN: 9788874581146.

P. SCARFATO, **M.L. FARIELLO**, L. DI MAIO, L. INCARNATO. Weatherability evaluation of nanocomposite polymeric treatments for surface protection of construction materials. Vth International conference on times of polymers (TOP) and composites. Hotel Continental Terme – Ischia, 20-23 June 2010. pp: 373-375, ISBN: 9780735408043.

L. DI MAIO, **M.L. FARIELLO**, L. INCARNATO, P. SCARFATO. Protezione di materiali lapidei mediante resine nanocomposite. IV Convegno "Monitoraggio e Conservazione preventiva dei Beni Culturali". Facoltà d'Ingegneria – Cassino, 27, 28, 29 Maggio 2010. Atti pp: 159-166, ISBN: 9788878680937

M. L. FARIELLO, P. SCARFATO, L. DI MAIO, L. INCARNATO. Innovative polymeric surface treatments for concrete protection. In: Le

nuove frontiere del calcestruzzo strutturale - The new boundaries of structural concrete. Università di Salerno, 22-23 Aprile 2010, ISBN/ISSN: 9788895028552

L. DI MAIO, **M.L. FARIELLO**, L. INCARNATO, P. SCARFATO. Surface Treatment of concrete with polymer/organoclay nanocomposite. 13th International Congress on Polymers in Concrete, 10 – 12 February 2010, Funchal – Madeira, Portugal; pp: 593 – 600, ISBN: 9789729917943.

Papers on International Journals:

P. Scarfato, L. Di Maio, **M. L. Fariello**, P. Russo, L. Incarnato (2011). Preparation and evaluation of polymer/clay nanocomposite surface treatments for concrete durability enhancement. CEMENT AND CONCRETE COMPOSITES, ISSN: 0958-9465. (In press).

M. L. Fariello, L. Incarnato, L. Di Maio, P. Scarfato (2010). *Surface treatment of concrete with polymer/organoclay nanocomposite*. RESTORATION OF BUILDINGS AND MONUMENTS, ISSN: 1864-7251, Vol (16), p. 325-330.

Table of contents

List of figures

List of tables

Abstract

In recent decades, the concrete for years considered unchangeable and with an unlimited life, with exceptional mechanical properties which have determined principally its success, was in fact subject to phenomena of degradation which over time alter its durability.

The degradation of concrete is hardly attributable to a single cause because often multiple processes can occur simultaneously, interacting in a synergistic way. Any degradation mechanism occurs, it is closely related to transport and diffusion of water in the concrete, i.e. the degree of porosity. Although the porosity of the concrete substrate is an intrinsic characteristic of the material itself, and therefore unavoidable, its control is crucial.

The protective polymer-based resins are the most commonly used for concrete structures, because they are very effective to provide a physical barrier to the ingress of water, ions and gases. Despite their good efficacy in prolonging the service life of the structures, there is a need for further increase the barrier properties and their compatibility with the substrate in aggressive environmental conditions.

In recent times, polymer-organoclay nanocomposites have emerged as a new class of high performance materials: in these systems nanoparticles are homogeneously dispersed in the polymer matrix in order to obtain an exfoliated structure. The high aspect ratio, which means a strong interactions between the nanofillers and the polymer, make the nanocomposites excellent organic-inorganic systems (compared to pure polymer or microcomposite systems), in terms of mechanical, thermal, optical and barrier properties.

This is the reason why, it has been thought to use these systems as potentially effective protective coating for building structures, even in the most severe environmental conditions.

In this thesis work different systems obtained by mixing a filler, in particular two kind of montmorillonite organically modified, with fluoro-based resins and silane-siloxane have been studied.

The protective efficacy of these systems, at different charge content has been verified and the results demonstrate the potential application of

polymer/organoclay nanocomposites as surface treatment materials for concrete structures.

Moreover, in literature very often the use of some additives such as micro and nanoparticles is studied because it is expected that both strength and durability of a concrete could be enhanced if the overall porosity is reduced. In particular in the last years different kinds of inorganic nanoparticles, due to their physical and chemical properties, are very often integrated with cement-based building materials; in fact, thanks to their high surface area to volume ratio they can react with calcium hydroxide ($Ca(OH)_2$) crystals, arrayed in the interfacial transition zone, and produce C–S–H gel which fills the voids to improve the density of the interfacial zone. Stable gel structures can be formed and the mechanical and the service-life properties of hardened cement paste can be improved when a smaller amount of nanoparticles is added.

On the other hand, the same hydrophobic agents used as surface protective, thanks to their capability in reduction significantly the molecular attraction between the water and the concrete, could be directly added in the concrete mix in order to make the whole concrete bulk hydrophobic.

Thus, in this work the research is aimed to investigate the separated and combined effect of a hydrophobic resin (silanes and siloxanes in water base) and of the nanoparticles (two montmorillonites organically modified, the Cloisite 30B and the Halloysite) on concrete durability in relation with the analysis of transport properties of cement based systems, not yet deepened in literature.

Chapter I
Introduction

I.1 Concrete degradation

Concrete, despite the excellent properties which have determined its success as a versatile and robust building material, can be severely weakened by poor manufacturing or a very aggressive environment. Thus, in the recent years, particular attention is being regarded to its durability, which has been defined by the American Concrete Institute [Papadakis 1991] as its resistance to weathering action, chemical attack, abrasion and other degradation processes. In other words, the durability of a concrete structure is the ability to withstand time, ensuring the service life for which the structure has been designed. The environmental attacks that influence the degradation mechanisms in concrete structures include the physical and chemical phenomena which can be classified as follows:

PHISICAL EFFECTS:

- Freeze-thaw damage
- Abrasion
- Mechanical loads

CHEMICAL EFFECTS:

- Alkali-aggregate reactions
- Sulfate attack
- Microbiological induced attack
- Corrosion of reinforcing steel embedded in concrete induced by carbonation of concrete and chloride attack.

In practice, the degradation mechanisms can act simultaneously with possible synergistic effects and are strongly related to water transport and diffusion in the material (Glasser 2007). In fact, it should be recognized that

concrete is intrinsically a porous material, and, despite the improvements on its formulation and quality control to the best possible extent, it is not possible to completely prevent the access of potentially harmful agents, such as chlorides, sulphates, carbon dioxide, and other pollutants which determine the increasing of decay rate and deterioration of concrete. In fact, the water required for concrete production the concrete, which is necessary for its workability and hydration, leave in the matrix, after maturation, a dense network of tunnels leading to the porosity of the cement paste, which is classified as gel and capillary porosity. The capillary porosity, which largely determines the intrinsic permeability of the cement conglomerate depends on the water/cement ratio, and the degree of hydration, and can range from 0 up to 40% in volume of cement paste. Moreover, micro-cracks and macro-pores, usually related to hygrometric contraction, will always exist in the concrete, providing a path for the transportation of water and gases. The mechanisms that determine the penetration of aggressive fluids in concrete are:

- *Permeation*: the aggressive penetration of the fluid is determined by a pressure gradient;
- *Diffusion*: entry into the porous medium is governed by a concentration gradient;
- *Capillary adsorption*: generated by the forces of adhesion surface affinity of a liquid, water in particular, with the surfaces of a solid (concrete)

As a result, both the durability and the engineering properties of concrete are directly related to transport properties which are influenced and controlled by the number, type, size and distribution of pores present in the cement paste, the aggregate components and the interface between the cement paste and the aggregate. Table I.1 lists the different porosity of concrete and their relative influence on the most common degradation processes of concrete.

Table I.1 *Concrete porosity*

CONCRETE POROSITY		
Type	**Dimension**	**Degradation effects**
Gel porosity	1 – 10 nm	Negligible
Capillary porosity	From 0.1 to 10 μm	Slow
Micro-cracks	Hundreds of μm	Medium/Fast
Macro-cracks	mm	Fast

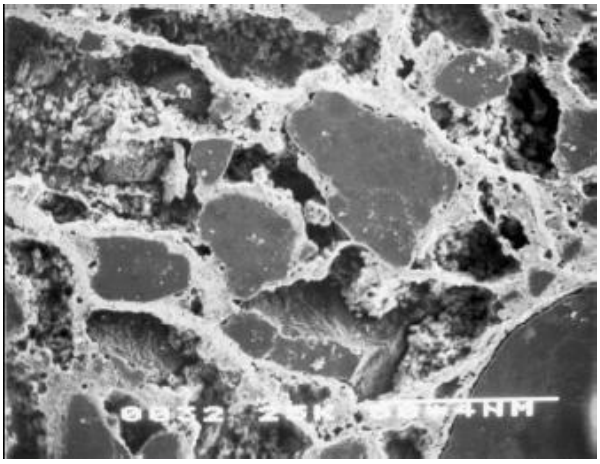

Figure I.1 *Optical microscopy of concrete sample.*

Usually in terms of interconnected pores, must be considered also the widespread presence of " incorporated or trapped air " in the fresh concrete, which should be expelled by a correct compaction of mix in order to avoid the formation of macro-voids (about 1 mm). Another variable that can increase both the porosity and the interconnection of the pores, can be found in the "transition zone", i.e. the cement paste layer (often a few microns or tens of microns) that is in direct contact with the aggregates.

I.2 Transport mechanisms in concrete

The transport of gases, liquids and ions through concrete is important because of their interactions with concrete constituents or the pore water, and thus it can alter the integrity of concrete directly and indirectly leading to the deterioration of structures as mentioned before. Depending on the driving force of the process and the nature of the transported matter, different transport processes for deleterious substances through concrete are distinguished as diffusion, absorption and permeation.

I.2.1Diffusion

Diffusion is the process by which matter is transported from one part of a system to another due to concentration gradient. The macroscopic movement occurs as a result of small random molecular motions, which take place over small distances. The progress of diffusion is much faster in gases than in liquids, solids being the slowest. Flux is a measure of diffusion which is the flow rate per unit area at which mass moves.

Fick's first law of diffusion, eq. (I.1), states that the rate of transfer of mass through unit area of a section, *J*, is proportional to the concentration gradient $\delta c/\delta x$ and the diffusion coefficient:

$$J = -D\frac{\delta c}{\delta x} \tag{I.1}$$

For non-steady state conditions, the concentration *c* at the location *x* changes with time, and the balance equation generally referred to as Fick's second law of diffusion, eq. (I.2), describes the change in a unit volume with time:

$$\frac{\delta c}{\delta t} = D\frac{\delta^2 c}{\delta x^2} \tag{I.2}$$

Here, *D* may be constant or a function of different variables, such as time, temperature, concentration, location, etc. For *D*=constant the solution of the above equation for the boundary condition of $c=c_{(0,t)}$ and the initial condition of $c=0$ for $x>0$ and $t=0$, is given by eq. (I.3):

$$C = c_0\left(1 - erf\left(\frac{x}{2\sqrt{Dt}}\right)\right) \tag{I.3}$$

where *erf* is the standard error function.

A factor to consider while dealing with the diffusion process is the chemical reactions taking place between the penetrating substances and concrete. For example, the diffusion of chloride ions into the concrete is accompanied by reaction such as physical and chemical binding at the hydration products. The reaction reduces the concentration of movable chloride ion at any particular site and, hence, the tendency for inward diffusion is further reduced.

In experiments, which do not explicitly consider binding, erroneous estimates are made using the diffusion eq. (I.2). Therefore, frequently an 'apparent' diffusion coefficient is deduced from experiments, which then depends on time *t* (Garboczi 1990).

I.2.2. Absorption

Transport of liquids in porous solids due to surface tension acting in capillaries is called water absorption. Absorption is related not only to the pore structure, but also to the moisture condition of the concrete.

The absorption of water into the dry concrete is considered to have two basic parameters:

1. the mass of water which is required to saturate the concrete (the effective porosity); and
2. the rate of penetration of the capillary rise (the sorptivity).

$$A = C + S\,t^{1/2} \tag{I.4}$$

where A is the term relating to the water intake, S the sorptivity, t the elapsed time and C is the initial disturbance observed by some researchers and is believed to be dependent on the surface finish (Basheer 2001).

Since the filling of capillary channels and voids and advancing of water occur almost side-by-side during absorption, a combined effect only can be measured, which will give a capillary effect.

I.2.3. Permeability

Permeability is defined as that property of a fluid medium which characterizes the ease with which a fluid will pass through it under the action of a pressure differential. Darcy's law, eq. (I.5), states that the steady-state rate of flow is directly proportional to the hydraulic gradient, i.e.

$$\upsilon = \frac{Q}{A} = -K\frac{\delta h}{\delta L} \tag{I.5}$$

where υ is the apparent velocity of flow, Q is the flow rate, A is the cross-sectional area of flow, δh is the head loss over a flow path of length δL and K is called the coefficient of permeability. Darcy's law has been generalized to apply to any fluid flowing in any direction through a porous material, so long as the conditions of flow are viscous.
The law can be expressed by the equation:

$$\upsilon = \frac{Q}{A} = -\left(\frac{k}{\mu}\right)\left(\frac{\delta P}{\delta L}\right) \tag{I.6}$$

where δP is the pressure loss over the flow path δL, μ is the viscosity of the fluid and the constant k is referred to the intrinsic permeability of the porous medium. Intrinsic permeability, with the dimensions of area, is the most rational concept of permeability, as it depends purely on the characteristics of the porous medium and is independent of those fluid characteristics which govern the flow, i.e. viscosity μ expressing the shear resistance of the fluid.

I.3 Strategies for concrete protection

Since the porosity represents the main characteristic of concrete structures, its control is fundamental in the production of a durable concrete. On the other hand, when it is not possible to modify the intrinsic porosity of

the concrete, it is necessary to protect the structures from the environmental attacks also performing, in some cases, a rehabilitation operation.

I.3.1 The protective treatments

The concrete structures are often subject to static loads, dynamic loads and variations in temperature or humidity, which can be due to tensile stresses, which, in a rigid material such as this, cause cracks. These are the gateway for air, water and other harmful agents. All this triggers the expansion and then the fracture, which proceed at an ever more high speed.

Within a few years appear cracks, delamination of concrete cover and reinforcement corrosion, signals clearly very dangerous.

The solution to the problem of cracks is in the protection of external surfaces of the artifacts.

I.3.1.1 The types of products

The existing product range is very wide. In market there are different types of materials for the protection of the concrete**,** among which we can make a first distinction: cement-based and polymer-based products.

The firsts are generally suitable for the application of thick layers of material (1 to 10 cm), while others are used in the form of thin coatings (1 to 2 mm) to protect concrete structures,

A further classification of the products on the market can be made based on the presence or absence of solvents in their composition. A distinction is made between products with solvents (sometimes harmful and/or flammable), those with little solvent, and those in aqueous solution. Of course the choice is made, as well as in relation to the type of application, even according to environmental conditions. In closed or at risk of fire because it would be recommended to use water-based compounds, which are also less polluting.

I.3.1.2 The product features

The many types of protective concrete, once applied, and after the crosslinking reaction of organic substances has occurred, become waterproof. The water then cannot penetrate the concrete, as well as acids and salts dissolved in the rain.

The continuous layer is formed, thus also protects from harmful and destructive effects of frost and thaw on.

The above water resistance and ability to isolate the aggressive gaseous compounds are necessarily accompanied by a breathable protective layer, in relation to the formulation of the product and the thickness of application. This is necessary because the moisture inside the pore surface should be

allowed to evaporate and escape over the coating, or it may create pressure that can cause detachment of the applied layer.

I.3.1.3 The composition

The composition of the products in action is being taken vary considerably, depending on different applications. Many of the plasters used epoxy resins or epoxy, because they are the most suitable for sealing cracks.

The liquid compounds such as paints rather prefer, as elastic component, acrylic resins Alkyd resins, polyacrylates and vinyl ones are applicable only as a simple finish.

The impregnating products, then, are generally characterized by the presence of silane in their composition. They are absorbed by the concrete and react by hydrolysis with moisture normally present in it. When cured, the outer surface, as well as the surface of the pores within which the silane is penetrated, is covered with a thin film of hydrophobic polymer. In general, all products have a chemical composition that resists in contact with the alkalinity of the cement-based substrates and ultraviolet rays.

Polymeric materials are organic molecules linked together, forming a chain or even a three-dimensional crosslinked structure. The polymerization usually takes place in situ. Very often they are two separate monomeric components which, when mixed together and applied on the media, react to produce the solid. Most commonly used resins of this category are represented by epoxy resins and polyurethane.

For polyacrylates and vinyl resins instead, the transformation of the monomer in the polymer has already been made prior to application. In this case the polymer is dissolved in an organic solvent or emulsified in water. The film is formed after the solvent is evaporated.

I.3.2 The modification of the mix concrete design

The concrete is often regarded as a material inevitably destined to cracking and degradation, despite the surface protection systems applied, which maintenance is often expensive and difficult. In theory, it would be possible to produce durable concrete (even when they are in hostile environments), provided that have been chosen the "ingredients" with appropriate characteristics, and subject to compliance with certain values of the water/cement ratio and volume of entrapped air in the dough. Under these conditions it is possible to produce a cement matrix of low porosity, which increases the durability of concrete.

The lack of pores in concrete corresponds to a significant slowing down of water penetration and, consequently, of aggressive agents in the conglomerate like carbon dioxide, sulfur dioxide, chlorides and so on.

It should be possible to select mixtures of raw materials for the production of concrete with various desired properties. In order to improve some of the properties of concrete, in the fresh state, very small quantities of chemical products were added into mix. These chemical admixture include: natural pozzolana, fly ashes, silica fume, calcareous filler and other fillers which are at least as fine as the particles of cement and sometimes much finer like nanoparticles. In fact nano-engineering, or nanomodification of concrete, is a quickly emerging field. The advantage of using nanoparticles is that they promote the hydration of cement and contribute not only to the strength of the concrete, but also to obtain a more reduced porosity of the system, very useful for the concrete protection, as mentioned above.

The concrete mix could be modified, in order to prevent the access of harmful agents, also making its bulk system completely water repellent by adding an hydrophobic resin inside, as discussed later.

I.4 Thermodynamic properties of concrete substrate

The repair materials used as surface treatments or as concrete additive must have not only suitable transport properties for the concrete protection, but must also present a physical and chemical compatibility with the concrete substrate.

The surface analysis is important to understand the interfacial phenomena between two interacting surfaces (Courard L. 2002), for example solid-liquid. A direct measurement of intermolecular forces is the surface free energy.

Studies on the properties of the surface layer of various materials, including the wettability and the surface free energy, are the subject of intensive scientific research for over forty years (Żenkiewicz M. 2007). These quantities are being assumed as important criteria for evaluation of adhesion properties of solids.

The most common method for the calculation of the surface free energy of solids, utilizing the results of the contact angle measurements obtained from the wetting property, comes from the Young Equation:

$$\gamma_{sv} = \gamma_{sl} + \gamma_{lv} \cos\Theta \qquad \text{(I.7)}$$

where γ_{sv} = surface energy of solid/vapor

γ_{sl} = solid/ liquid interfacial free energy

γ_{lv} = surface energy of liquid/vapor

Θ = contact angle

In Figure I.2 is reported the contact angle of a liquid sample on a solid surface surrounded by vapor.

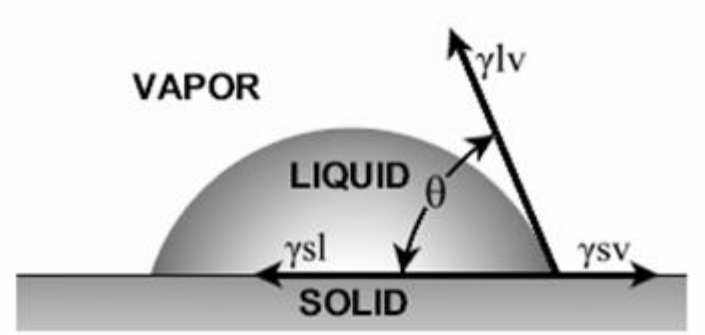

Figure I.2 *Wetting conditions of a solid by a liquid*

In this work a large space was given to the measurements of contact angle in order to have an interpretation of surface quality as well as of the hydrophilicity of treated and untrated cementitious materials.

I.5 Background

The recent strategies of concrete protection are mainly based on surface treatments by making use of water repellent and impermeable materials which allow to realize a physical barrier between the concrete and the environment; it being understood that these materials must have a physico-chemical compatibility with the concrete substrate. This topic represents the object of study in several literature works which have been developed in the last few years, with a particular regard to the application of polymeric resins in the concrete protection and durability enhancement.

The surface protection materials for concrete can be classified into three groups:

- pore liners (make the concrete water repellent),
- pore blockers (form insoluble products in the concrete pores) and
- coatings (form continuous film on concrete surface).

Figure I.3 illustrates these three groups of protection.

The impregnating products have special characteristics that do not form a film on the surface, but penetrate into the pores and capillaries of the material forming within them a hydrophobic layer.

Recent studies (Almusallam 2003, Vipulanandan 2005) have shown encouraging results on the performance of surface treatments with coatings, sealers or pore liners which are an effective way to prolong the life of structures. However, with a wide range of coatings available in the market, it becomes extremely difficult to choose the right product, since similar generic types are known to possess considerably different characteristics.

In the following, some literature examples of using polymeric resins as protective coatings are presented.

Madeiros et al. (2009) studied the efficacy of certain surface treatments (such as hydrophobic agents, acrylic coating, polyurethane coating) in inhibiting chloride penetration in concrete. All surface treatments reduced the capillary water absorption compared to the reference (minimum = 73% and maximum = 98%). The results indicated that the most efficient protection system could reduce the chloride diffusion coefficient of concrete by 86%.

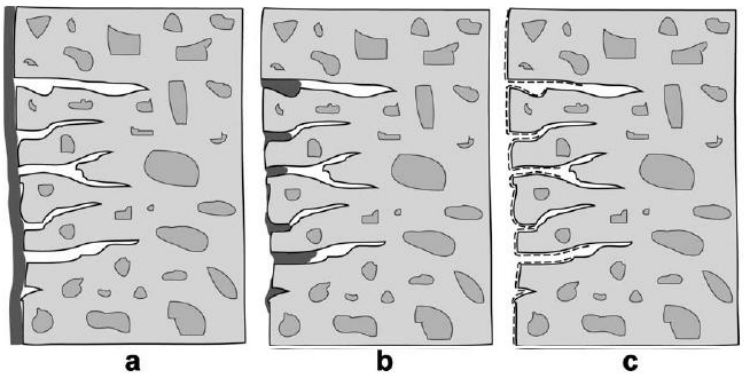

Figure I.3 *Groups of surface treatments: (a) coating and sealers (b) pore blocker (c) pore liner*

Sergi et al. (1990) studied the influence of surface treatments on corrosion rates of steel in carbonated concrete and concluded that water-repellent surface treatments that line the pores of concrete with hydrophobic layers, were effective against water penetration and limiting the corrosion rate of steel in carbonated regions in the specimens exposed to cycles of wetting and drying. The compatibility and the adhesion of some epoxy resin-based coatings to the concrete substrate were studied by some authors (Dulaijan et al. 2000). The performances of epoxy based coatings resulted to better when compared to some acrylic resin-based surface coatings. In any case both materials considerably reduced the diffusion of carbon dioxide into the concrete matrix. Ibrahim et al. (1999) evidenced the protective performance of silanes, silanes/siloxanes and acrylic coatings. Park (2008) has examined the effects of the degradation of coatings during a concrete carbonation test. Moreover, he has constructed a diffusion-reaction carbonation model which allows to estimate long-term carbonation, taking account of the degradation with time of surface finishing materials, especially organic coatings.

More recently, polymer-nanoclay composites have emerged as a new class of advanced organic-inorganic materials with excellent mechanical properties and barrier characteristics with only a few percent of well-

dispersed clay reinforcement. These materials demonstrated that it is possible to sensibly enhance barrier properties with particular regard to water and vapour permeability of some resin based coatings (Vacchiano 2008).

However, only few works are aimed to study the behaviour of these materials in relation to the durability of concrete. Some recent results (Leung et al. 2008) indicate significant improvement in moisture penetration resistance when small amount of organoclay, ranging from 1 to 5 wt%, are introduced into epoxy and silane based coatings (Figure I.4).

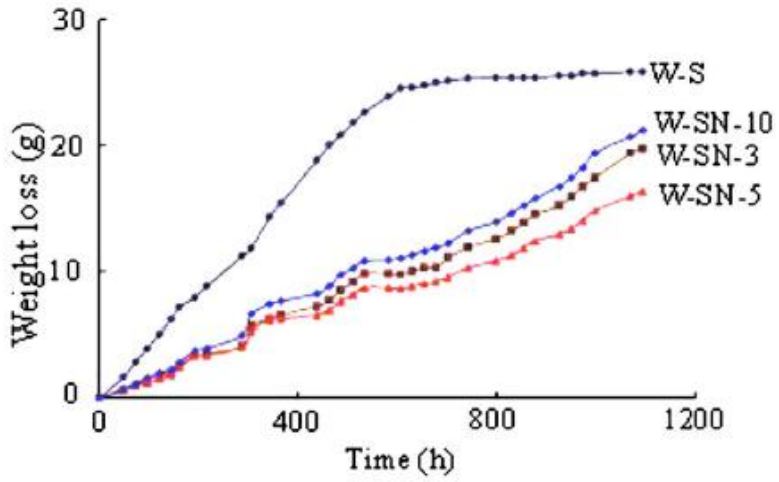

Figure I.4 *Weight loss versus time for silane treated specimens layered at different amount of organoclay (3-5-10wt %)*

Some investigations on the environmental degradation mechanism of epoxy-organoclay nanocomposites due to accelerated UV and moisture exposure (Woo 2007) have highlighted that the nanocomposites coatings exhibit smaller cracks with a less degree of discoloration than the neat epoxy. Moreover, the same authors (Woo 2008) evaluated the residual mechanical properties of epoxy-organoclay nanocomposites after UV exposure. Also in this case, the results confirmed the beneficial effects of organoclay: the tensile modulus increased with increasing clay content at the expense of reductions in failure strain; after UV exposure there were only negligible changes in tensile modulus, while the tensile failure strain was significantly reduced with UV exposure time due to the embrittlement effect, and the addition of organoclay mitigated the failure strain reduction

Other authors (Selvaraj 2009) have found a suitable protective coating to steel rebar to improve the durability of such structures under aggressive exposures, as marine environments.

Some surface treatments of natural tuff stone with nanocomposites based on fluoroelastomers and acrylic polymers were already studied by our research group, with very encouraging results (D'Arienzo 2008). For this reasons part of the experimental work of the present thesis was aimed to investigate the extent of the better moisture barrier performance of nanocomposites and to verify their effectiveness as protective coatings for the concrete.

In the construction field the modification of cement with nanoparticles is a rapidly growing phenomenon, as just said. In fact nanosized particles having a high surface area to volume ratio which provides a considerable chemical reactivity, can act as nuclei for cement phases, further promoting cement hydration (Sanchez 2010). In the literature many authors have utilized as nanosized additives the nano-silica (SiO_2) (Ji 2005; He 2008) and the nano-titanium oxide (TiO_2) (Marwa 2010). Only few works are about the incorporation of nano-iron (Fe_2O_3) (He 2008), nano-alumina (Al_2O_3) (Li 2006) and nanoclay particles (Kuo 2006, Fernandez 2011). The majority of these works have been interested in studying the mechanical properties of the systems modified with the addition of nanoparticles (Shebl 2009) emphasizing the effectiveness of the nanoparticles in promoting the hydration of cement leading to better mechanical properties. However, nanoparticles, promoting the hydration of cement, also induce a reduction of porosity in cement paste (Sanchez 2010), obstructing the passage of external chemical agents. So, the nanoparticles could be utilized as additive for concrete in order to ensure a more durable concrete.

Another important strategy to prevent the deterioration of a concrete is to make it impermeable to the inlet of water which is considered the main vehicle for aggressive substances.

The hydrophobic agents, thanks to their capability in reduction significantly the molecular attraction between the water and the concrete, can be applied as surface treatments (Medeiros 2009; Almusallam 2003) in order to provide a physical barrier between the substrate and the surrounding environmental or can be directly added in the concrete mix in order to make the whole concrete bulk hydrophobic (Tittarelli 2010; Aldred 2001)

I.6 Aim of the work

In this PhD thesis the research is aimed to investigate the effect of the clay such as montmorillonite organically modified added to the concrete mix, on the durability properties of cement mortars.

Therefore, during the first year of the present PhD work, attention was paid to the concrete protection strategies and to the effect of surface coatings on the transport properties of concrete samples. A preliminary experimental analysis of innovative polymeric based surface treatments for the concrete protection against the environmental attacks was then carried out.

In the second year further investigations were carried out to analyze the efficacy of all protective systems (nanocomposites and not) on durability of concrete samples pointing the attention on the understanding of the relations between the improved performance of the treated samples and the different character of the two polymeric resins examined through qualitative and quantitative analyses with particular regard to porosity measurements and transport properties. Moreover, the study on the effects of the UV degradation of nanocomposites polymeric treatments has been carried out.

In the third and last year, starting from the results of the previous work and supported by literature, a new concrete mix has been realized by adding two ingredients: an hydrophobic resin to make the whole system hydrophobic and two types of nanoparticles (platelet and tubular) to modify the porosity of the concrete. The concrete systems with the different combinations of these additive were studied from the transport properties point of view. The modeling of some data has been also done. Moreover in order to detect the possible presence of cracks within the samples, and then to determine in a quantitative way the mechanical properties during early stages of hardening of concrete samples, the analysis of dynamic modulus and of compression resistance has been carried out

Chapter II
Experimental

II.1 Materials

II.1.1 Concrete specimens

The concrete and the mortar samples are produced with a Portland cement designated CEM II A-LL 32.5R which is equivalent to UNI EN 197-1 (2007) requirements.

The blend proportion of the concrete was 1.0 (cement): 2.7 (sand): 0.5 (fine aggregate): 2.2 (coarse aggregate) and water/cement ratio was equal to 0.53.

During the molding of concrete specimens a vibrating needle was used to ensure proper compaction.

The molds were removed after 24 hours and all specimens were cured for 28 days at 25 °C and 90% R.H.

II.1.2 Surface protection materials

Two types of polymeric resins commercially named as Fluoline CP supplied by CTS s.r.l. (Altavilla Vicentina – VI, Italy) and Antipluviol S supplied by MAPEI s.p.a. (Milano, Italy) were used as protective agents.

Fluoline CP is a blend of an acrylic polymer and a vinylidenfluoride based polymer in acetone solution. Fluoline CP is characterized by easiness in the use and good reversibility (i.e. it is removable) in acetone. Antipluviol S is a colorless liquid based on silane/siloxane resins in solvent solution normally used for exposed concrete structure.

Both solutions are characterized by low viscosity which make them able to penetrate the concrete pores and to form a continuous polymeric layer without altering the appearance of the manufact.

The application was made by brush following the recommendations of the supplier on 28 days cured concrete specimens.

II.1.3 Hydrophobic resin additive

A commercially resin named as Antipluviol W supplied by MAPEI S.p.A. (Milano, Italy), was used as hydrophobic resin. Antipluviol W is a milky, silane and siloxane-based dispersing agent in watery emulsion, characterized by its high capacity to penetrate all absorbent mineral materials used in the building industry to make them water repellent. Table II.1 shows the specific properties of the selected concrete coatings and of the hydrophobic agent chosen as additive, as reported in the technical sheet.

Table II.1 *Properties of polymeric coatings*

	Fluoline CP	*Antipluviol S*	*Antipluviol W*
Description	Consolidant/protective, completely reversible in acetone	Impregnant water-repellent	Water-repelling agent
Chemical composition	Blend of ethylmethacrylatemethylacrylate copolymer and of vinylidene fluoride-hexafluoropropene copolymer in solvent solution	Silane/Siloxane resins in solvent solution	Silane/Siloxane-based hydrophobic agent in water emulsion
Aspect	Transparent liquid	Transparent liquid	Milky liquid
Drying time (at 23° C)	About 10 h	About 1 h	About 1 h
Specific Weight [Kg/l]	0.81 ± 0.03	0.83 ± 0.03	1.01 ± 0.03
Dry solids content [% wt/wt]	3.7	7.5	8

II.1.4 Nanoparticles

Two kinds of nanometric particles have been chosen to add into the resins: *Cloisite 30B* which is a layered sodium montmorillonite organically modified by N,methyl-N,tallow-N,N0,2-hydroxyethyl-ammoniumchloride (90 meq/100 g clay), supplied by Southern Clay Products, and the *Halloysite* which is an aluminosilicate clay which is characterized by a tubular

morphology. Its chemical formula is $Al_2Si_2O_5(OH)_4 \cdot H_2O$. Prior to any use, the silicate nanoparticles were dried in a vacuum oven at 90°C for 24 h to obtain a low level of residual moisture.

II.2 Methods

II.2.1 Coated concrete systems

Preparation of polymer/organoclay mixture

Nanocomposite systems based on Fluoline CP and Antipluviol S resins were obtained at different loadings of Cloisite 30 B (0, 2, 4 and 6 wt%). The required amount of organoclay was first added to resin with mild stirring until the powder uniformly dispersed in polymeric solution without any visible agglomerate. The polymer/organoclay mixture was subsequently sonicated for 1 hour in ultrasonic bath at room temperature to achieve satisfactory dispersion and to promote the exfoliation process of organoclay in the polymeric matrix. Some film samples of all resins were produced through solvent casting at room temperature.

The sample nomenclature used for discussion of the results is detailed in Table II.2 and Table II.3.

Effective intercalation/exfoliation of the organoclay via the above process was proved by X-ray diffraction analysis performed on film samples of each mixtures.

Table II.2 *Sample film nomenclature*

Film Nomenclature	Description
CP	Neat Fluoline CP resin
CP-30B 2%	Fluoline CP blended with 2 wt%of Cloisite 30 B
CP-30B 4%	Fluoline CP blended with 4 wt%of Cloisite 30 B
CP-30B 6%	Fluoline CP blended with 6 wt%of Cloisite 30 B
AS	Neat Antipluviol S resin
AS-30B 2%	Antipluviol S blended with 2 wt%of Cloisite 30B
AS-30B 4%	Antipluviol S blended with 4 wt%of Cloisite 30B
AS-30B 6%	Antipluviol S blended with 6 wt%of Cloisite 30B

Table II.3 *Sample concrete nomenclature*

Concrete Nomenclature	Description
CLS	Untreated concrete sample
CLS+CP	Concrete paint-brushed with neat Fluoline CP resin
CLS+CP-30B 2%	Concrete paint-brushed with the Fluoline CP + Cloisite 30B 2 wt% system
CLS+CP-30B 4%	Concrete paint-brushed with the Fluoline CP + Cloisite 30B 4 wt% system
CLS+CP-30B 6%	Concrete paint-brushed with the Fluoline CP + Cloisite 30B 6 wt% system
CLS+AS	Concrete paint-brushed with neat Antipluviol S resin
CLS+AS-30B 2%	Concrete paint-brushed with the Antipluviol S + Cloisite 30B 2 wt% system
CLS+AS-30B 4%	Concrete paint-brushed with the Antipluviol S + Cloisite 30B 4 wt% system
CLS+AS-30B 6%	Concrete paint-brushed with the Antipluviol S + Cloisite 30B 6 wt% system
CLS+AS-H 2%	Concrete paint-brushed with the Antipluviol S + Halloysite 2 wt% system
CLS+AS-H 4%	Concrete paint-brushed with the Antipluviol S + Halloysite 4 wt% system
CLS+AS-H 6%	Concrete paint-brushed with the Antipluviol S + Halloysite 6 wt% system

XRD examination

X-ray diffraction measurements (XRD) were performed on nanocomposites films and clay powder with a Rigaku D/MAX -2000 Diffractometer using a Ni-filtered Cu-Kα radiation (40kV, 20mA).

TEM and SEM analyses

Transmission electron microscopy (TEM) analysis was conducted using a Philips EM 208 with different magnification levels. The images were get on ultrathin specimens obtained with a Leica Ultracut UCT microtome. Concrete samples were also observed by a scanning electron microscope (SEM) model LEO 420. Before analyses the samples were covered with 250 Å of gold-palladium using a sputter coater (Agar model 108A).

Differential scanning calorimetry (DSC)

Differential scanning calorimetry measurements (DSC) were carried out using a Mettler DSC-30, in the temperature range of -70-300°C, in nitrogen atmosphere.

Thermogravimetric analyses

Thermogravimetric analyses (TGA) were performed using a Q500 analyzer in nitrogen atmosphere in the temperature range of 25-900°C.

Water vapor transmission test

The permeability to steam is defined as the amount of water vapor flowing during the time unit and through the surface unit of the sample.

In this study, the steam transmission tests were performed according to the wet method specified in ASTM E96-95 (1995), in which a water vapor pressure gradient is applied through the thickness of thin concrete plate specimen to determine the moisture transmission rate. Test setup for water vapour transmission test is reported in Figure II.1.

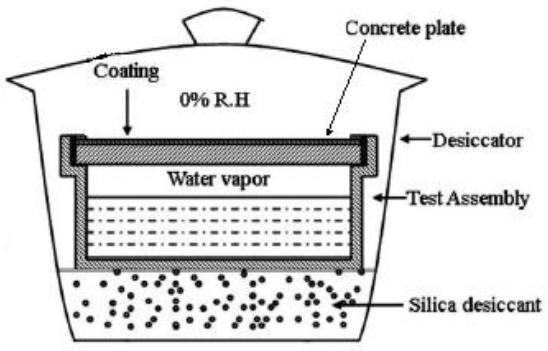

Figure II.1 *Test setup for water vapor transmission test*

Samples thickness was 1 cm and the steam exposed area was fixed at 38.5 cm^2. The weight loss of the test assembly (i.e. the water vapor which crosses the specimen) was recorded at intervals of 24 hours and the measurement was continued until a steady state weight loss had been reached.

The water vapor transmission rate (WVT) and the water vapor diffusion coefficient *(D)*, which is a material constant, were calculated using respectively the following eqs. (II.1) and (II.2):

$$WVT = \frac{\Delta M}{T \times A} \qquad \left[\frac{g}{h \cdot mm^2}\right] \tag{II.1}$$

where WVT = water vapor transmission rate; ΔM = steady-state weight change; A = exposed area to water vapor; T = time.

$$D_T = \frac{WVT \times t_T}{P_W} \qquad \left[\frac{mm^2}{h \cdot}\right] \tag{II.2}$$

where D_T = water vapor diffusion coefficient of samples; t_T = total thickness of specimen; P_W = density of saturated water vapor at the test temperature, which equals 23 g/mm^3 at 25°C.

Contact angle measurements

Static contact angle measurements were performed with a contact angle system FTA 1000 instrument (First Ten Angstroms, Inc.). Tests were carried out on nanocomposites films and on samples of concrete untreated and treated with protective resins.

Sulphates attack

Cement-based materials exposed to sulfate solutions such as some natural or polluted ground waters (external sulfate attack), or by the action of sulfates present in the original mix (internal sulfate attack) can show signs of deterioration. Sulfate ions react with ionic species of the pore solution to precipitate gypsum ($CaSO_4.2H_2O$), ettringite ($[Ca_3Al(OH)_6 \cdot 12H_2O]_2 \cdot (SO_4)_3 \cdot 2H_2O$) or thaumasite ($Ca_3[Si(OH)_6 \cdot 12H_2O] \cdot (CO_3) \cdot SO_4$) or mixtures of these phases. The precipitation of these solid phases can lead to strain within the material, inducing expansion, strength loss, spalling and severe degradation.

The sulphates attack tests carried out on brushed samples were made according to the ASTM C88-05 (2005) procedure. It consists in cycles of immersion in a saturated solution of sodium sulphate (Na_2SO_4) and drying in oven to constant weight. The evaluation of sulphate attack was made by measuring the samples weight variation along a total of eight cycles. For coated specimens, due to the low heat resistance of polymeric resins, the temperature of the oven was set at a lower one (Aguiar 2008): in our case the treated specimens were dried at 75±5°C while untreated specimens were dried at 110 °C.

Sulphates which are carried into the inner sections of concrete by either ionic diffusion or capillary absorption may react with the cement constituents (as specified above) and cause destructive forces leading to cracking of the concrete.

Colorimetric Analysis

In order to evaluate the variation of the aesthetical properties induce by treatments, colorimetric analysis was carried out on the untreated and treated concrete samples with a CR-410 HEAD colorimeter (Konica Minolta Sensing, Inc.), based on the *L**, *a** and *b** coordinates of the CIELAB space, following the Italian Recommendation NORMAL 43/93 (1993).

ATR FT-IR analysis

ATR FT-IR analyses were carried out using a Nexus Thermo-Nicolet spectrophotometer, in the frequency range of 4000-650 cm^{-1}.

UV weathering

Weathering experiments were performed exposing the samples to UV radiation for 7 days in a climatic chamber at 25°C and R.H.= 50%; at the end of this period the samples were photographed, to compare their chromatic appearance with that of the unaged ones, and resubmitted to ATR FT-IR tests.

Porosimetry

The pore structure of the concrete samples was investigated by mercury intrusion porosimetry technique with Pascal 140 and Pascal 240 (Thermo Finnigan) instruments. The pressure range of the porosimeter was from subambient up to 200 MPa, covering the pore diameter range from about 0.007 to 100 μm. Values of 141.3 and 480 Dyne/cm were used for the contact angle and mercury surface tension.

Tests were carried out on small-cored samples with dimensions 2x1x1 cm^3 taken out from the concrete cubes (7x7x7 cm^3). The samples were dried in an oven at 60°C overnight and stored in a dessicator until testing. Mercury intrusion porosimeter tests were carried on five numbers of each sample to ensure adequate accuracy of the results (about 15%).

II.2.2 Hydrophobic and nanocomposite systems

Concrete and mortar samples production

For the nanocomposite concrete and mortar samples production the cloysite C30B, before adding it in the mortar and concrete mixture, it has been mixed in part of the stoichiometric water necessary for the cement past mixing with the help of a surfactant to let a good dispersion and segregation of the aggregated cluster, while for the hydrophobic-nanocomposite concrete and mortar samples production the nanoparticles of cloysite are mixed in the hydrophobic resin always with the help of a surfactant.

In the following, in Table II.4 and Table II.5, is reported the legend used for every sample analyzed in this work.

In particular the mortars and concrete samples are referred as X_Y, where X is the amount percentage of the resin Antipluviol W, whereas Y is the weight percentage of Cloisite 30B nanoclay (Table II.4) or the percentage of Halloysite (Table II.5).

Table II.4 *Legend of samples loaded with Cloisite C30B*

Samples Name	X Dry polymer [%wt]*	Y Clay C30B [%wt]*
CLS (0_0)	0	0
0_0.5	0	0.5
0_1	0	1
0_2	0	2
1_0	1	0
1_0.5	1	0.5
1_1	1	1
1_2	1	2

*Percentage respect the cement amount

Table II.5 *Legend of samples loaded with Halloysite*

Samples Name	X Dry polymer [%wt]*	Y Halloysite [%wt]*
CLS (0_0)	0	0
0_0.5H	0	0.5
0_1 H	0	1
0_2 H	0	2
1_0 H	1	0
1_0.5 H	1	0.5
1_1 H	1	1
1_2 H	1	2

*Percentage respect the cement amount

Water adsorption test

According to UNI 7699 (2005) the water adsorption test is conducted on concrete specimens, after weighted, immersed in a box filled of water at room temperature and at atmospheric pressure. Each sample is removed from water every 24h, wiped off with a damp cloth and weighted. The test continues until there is no variation mass greater than 0.1% between two consecutive weighing.

Similar test is conducted also under vacuum following the standard UNI 9526 (1989). From this two tests is possible calculate respectively the open porosity defined as the ratio between specific volume and water adsorption, and the accessible porosity as the ratio between specific volume and water adsorption under vacuum.

Capillary sorption test

The capillary water adsorption test is carried out following the European Standard UNI EN 772-11 (2006). The test is performed by exposing prismatic specimens to liquid water on one of the plane ends and by measuring, as a function of time, the increase in the mass resulting from the absorption of water. Specimens were placed in a pan where the fluid level was maintained at a constant height of 5 mm throughout the experiment. The amount of fluid absorbed was then calculated and normalized by the cross-section area of the specimen exposed to the liquid.

The sorptivity coefficient (CA) corresponds to the slope of the resulting approximating straight line reported in function of the squared root of the time. Mass variation are registered until the samples saturation is reached.

Oxygen Permeability test

On the concrete samples is carried out also the Oxygen Permeability test according to the UNI 11164 (2005). In Figure II.2 test cell and the wholly apparatus test are reported.

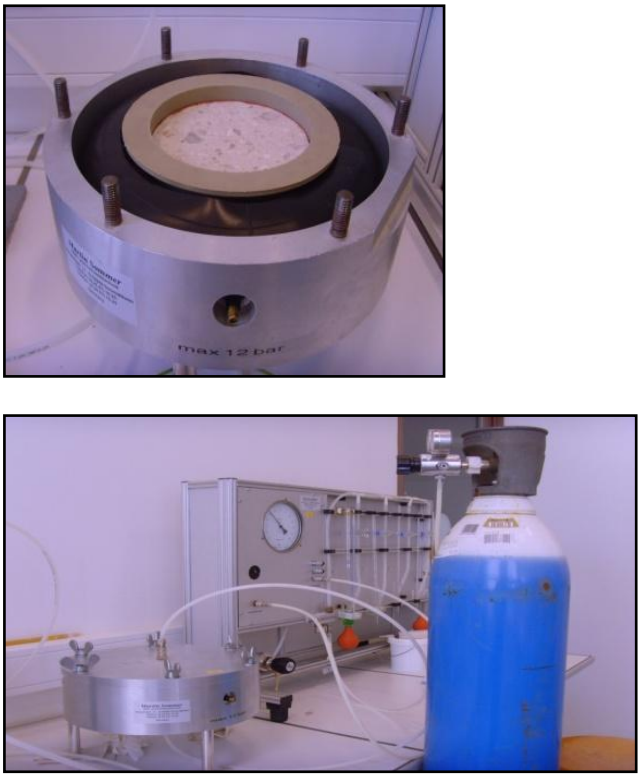

Figure II.2 *Test cell and apparatus for Oxygen Permeability test*

The sample placed in the test cell is subjected to a pressure difference equal to ΔP 2, 3, 4 and 5 bar. The Poiseuille formula, eq. (II.3), is used to calculate an apparent permeability:

$$k_{app} = \frac{2\,Q\,P_a\,L\,\eta}{A(P^2 - Pa^2)} \qquad \text{(II.3)}$$

where: Q is the flow measured in m^3/s
P_a is atmospheric pressure (10^5N/m)
L is the thickness of the specimen in m,
η is the viscosity of oxygen at the test temperature, 20 ° C ($2.02 \cdot 10^5$ Ns/m)
A is the section of the specimen in m,
P is the absolute pressure imposed on the basis of the sample in N/m^2.

Klinkenberg has developed a theory, eq. (II.4), according to which the relationship between the apparent permeability and the inverse of the average pressure is linear, the average pressure is the average between atmospheric pressure and absolute pressure. This relationship is expressed by two parameters, k_{int} and β:

$$k_{app} = k_{\text{int}}\left(1 + \frac{\beta}{P_m}\right) = k_{\text{int}} + k_{\text{int}}\frac{\beta}{P_m} \qquad \text{(II.4)}$$

At the end of measurements, a value of k_{app} apparent permeability is obtained for each value of pressure ΔP. The equation of the linear regression on the points of the graph {k_{app} vs $1/P_m$} determines a value of k_{int} for each sample. Since three samples were tested for each composition, three values of intrinsic permeability will be determined for each of them.

Carbonation resistance test

The determination of carbonation resistance is carried out following the standard UNI EN 13295 (2005). The test is performed on rectangular specimens, 40 mm x 40 mm x 160 mm. Three specimens were tested by composition. Demolded the day after the production, the specimens are then stored 28 days under water in the moist chamber. Then they are placed in the laboratory (20°C, 65% RH) until constant weight (mass change less than 0.2% in 24 hours). The specimens are then ready to be putted in the CO2 chamber and are positioned vertically, spaced 20 mm. The concentration of CO2 in the oven is 1 %, the temperature is 21 (± 2)°C and the relative humidity is about 60 (± 10)%. In Figure II.3 the specimen and the equipment for this test are reported.

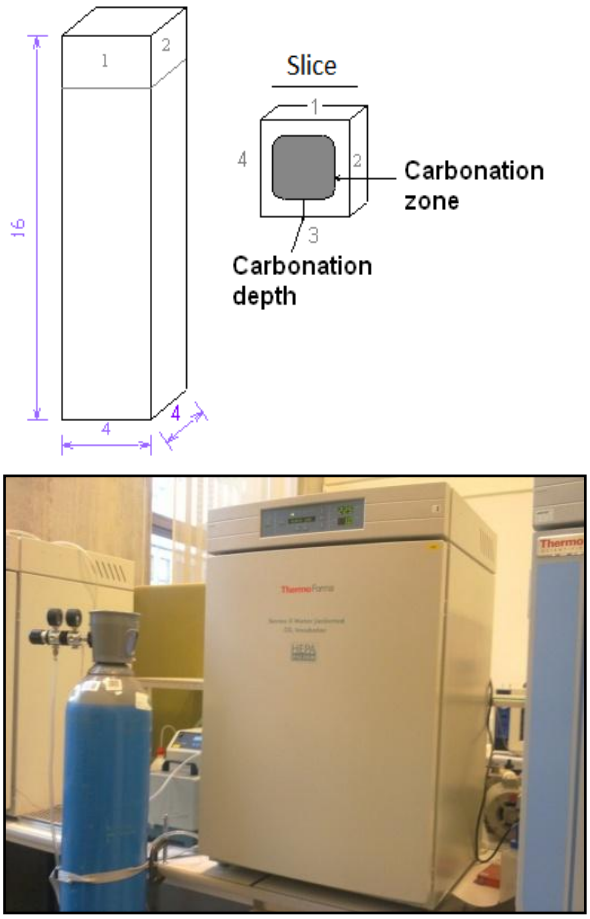

Figure II.3 *Test sample and equipment for carbonation resistance test*

Each month after the introduction of specimens in the CO2 chamber, a slice of 20 mm of the sample is sawed and analyzed. The inner face of the cut specimen is sprayed with a solution of phenolphthalein. The next day, the carbonation depths were determined and expressed in mm. Samples are stored for comparison to the following one month later.

Chloride diffusion test

To determine how the mortar passes chlorides, a diffusion cell was constructed in accordance with UNI CEN/TS 12390-11 (2010). The cell for the chloride diffusion test consists of a slice of mortar surrounded on both sides by two cylindrical Plexiglas compartments of 56 mm internal diameter (∅) and 90 mm in length (L) containing one, a water solution of limewater ($Ca(OH)_2$), and the other a solution of limewater saturated with chlorides

($Ca(OH)_2$ + NaCl 3 M) and the whole is glued (Figure II.4). Part of the mortar that is outside the cell is coated with epoxy resin to prevent exchange with the environment. At a specific time from the cell don't containing chlorides initially, will be determined the chloride concentration which is passed through the mortar.

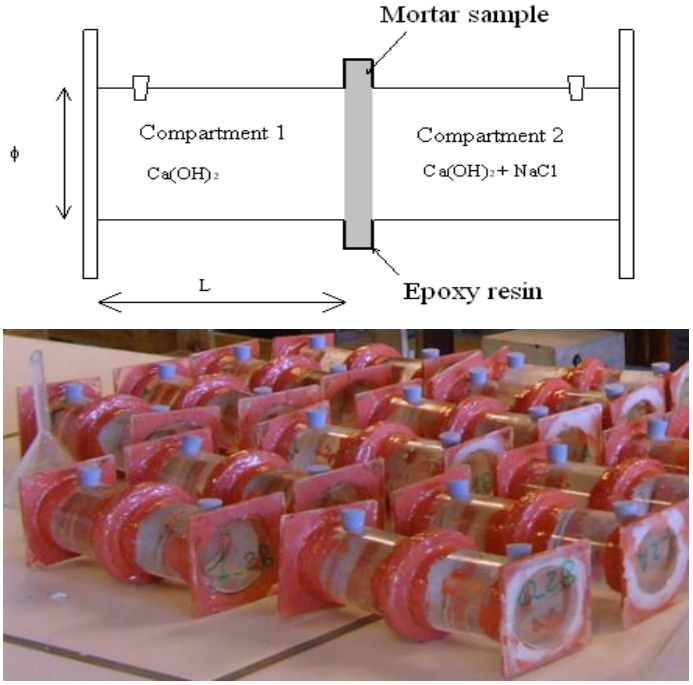

Figure II.4 *Test setup for Chloride diffusion test*

Sulphates attack

To determine the action of sulphates on the mortars, according to the standard ASTM C1012-95, specimens are immersed in a solution of sulphates and others of the same composition in deionized water (which will serve as referring). Their length is measured monthly and any degradation is observed. The comparison between the specimens remained in the water and those placed in sulphates is the hallmark of the action of sulphates.

Determination of Dynamic Modulus of Elasticity

The elastic modulus of a concrete sample is one of the most important properties to related to the physical state. The value of the elastic modulus in concrete usually ranges between the aggregate modulus and that of the cement paste. The value of the elastic modulus can be measured directly by detecting the deformation caused by loads (static modulus) or through

measurements of other properties (dynamic modulus) such as the propagation velocity of ultrasonic pulse through the material.

The formula proposed by the UNI EN 12504-4:2005 which yields the dynamic modulus of elasticity is:

$$E_d = V \cdot \rho \cdot [(1+\gamma_d)+(1-2\gamma_d)]/(1-\gamma_d) \quad \text{(II.5)}$$

where E_d = dynamic modulus of elasticity of the medium, in Pascal;
V = velocity of propagation of ultrasonic waves in m / s;
ρ = bulk density, in kg/m^3;
γ_d = Poisson's ratio of the dynamic medium.

The frequencies of mechanical vibrations used in concrete and similar materials are between 25 KHz and 200 KHz. The velocity measurement of the propagating waves can be made by reflection or transmission, which requires the use of a device comprising: a piezoelectric transmitting probe placed in contact with the concrete surface which sends ultrasonic waves; a receiving probe which collects the ultrasonic waves and converts them into an electrical signal; the detection unit, that is connected to the probes measuring the transit time.

The speed of propagation of ultrasound is calculated based on the transit time of ultrasonic pulse and on path length (distance between the transmitting and receiving probes) of the sound with the equation: V = L / t where V = velocity of ultrasound (m / s), L = path length (m), t = transit time (s). So the ultrasonic transit velocity turns out to be an indirect measure.

The speed of propagation inside the medium is mainly depending on: the quality of the concrete (the higher the class, the greater the V), the manner in which it was thrown (well vibrated concrete, concrete with no discontinuities due to gravel, right dosage), and the presence within it of discontinuities, cracks. Test equipment and setup for Dynamic Modulus of Elasticity are reported in Figure II.5.

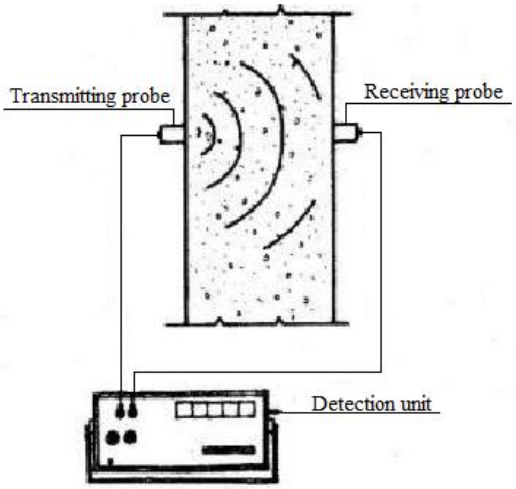

Figure II.5 *Test setup and equipment for Dynamic Modulus of Elasticity test.*

Resistance Compression Test

The samples subjected to ultrasonic investigations, after two months of maturation, were subjected to crushing tests to determine the compressive strength.

The UNI 12390-3 provides requirements to follow to determining the resistance to compression provided by cubic samples (or cylindrical) of hardened concrete. The test consists in subjecting a specimen of concrete to a compressive load (using a hydraulic press of adequate power) which

increases at a constant speed, until the maximum value of breakage is reached.

The concrete cubic samples used in this test are of size 150*150*150 mm^3.

Once located the specimen in the center of the plates of the press, a load is applied which increases at a constant speed until the breaking of the specimen is reached; The software of the apparatus returns the value of the breaking load F (N) and dividing by the area A (mm^2) of the specimen in contact with the plate of the press, we obtain:

$$\sigma = \frac{F}{A} = \left(\frac{N}{mm^2} \right) = (MPa) \qquad \text{(II.6)}$$

where σ is the compression resistance.

Chapter III
Results of treated concrete samples characterizations

III.1 Treatments characterization

Organoclay based nanocomposite systems are characterized by the exfoliated/intercalated state of the clay in the polymeric matrix. Such a state is essential for the properties development of the nanocomposite. In order to verify that the Cloisite 30B achieved a proper nano-dispersion level into the polymeric resins, SAXD measurements were carried out both on the neat silicate powder and on films of Fluoline CP and Antipluviol S at different organoclay content (2, 4 and 6 wt%).

As shown in Figure III.1, the characteristic basal reflection of the Cloisite 30B centered at about 2θ= 4.9° corresponding to a d-spacing of 1.8 nm, in the SAXD profiles of all the hybrid films appears broadened and shifted at lower 2θ angles.

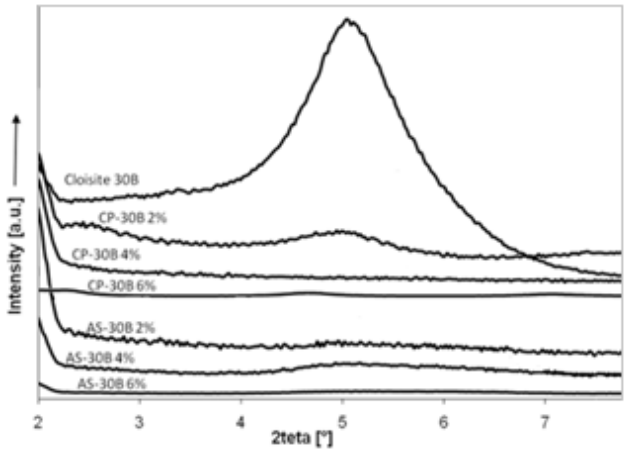

Figure III.1 *SAXD profiles of neat Cloisite 30B and of Fluoline CP and Antipluviol S cast films at different organoclay content*

These results suggest that the interlayer distance of the organoclay has increased with both polymeric resins, that is, intercalation/exfoliation of the clay has occurred, as confirmed also by TEM analysis.

As an example, in Figure III.2 is reported the TEM micrograph of the sample CP-30B 4%.

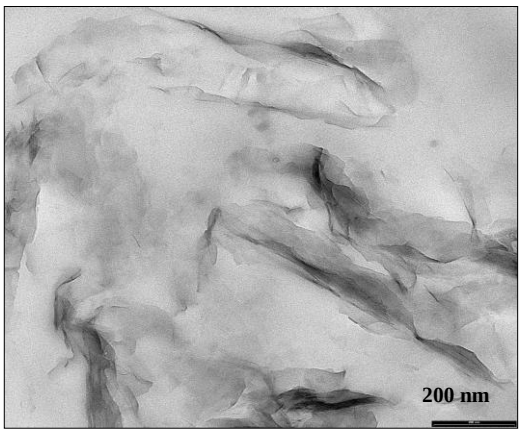

Figure III.2 *Example of TEM micrograph of the sample CP-30B 4%*

The effect of the obtained nanoscale dispersion of the filler on the thermal behavior of the polymeric systems was investigated by means of DSC and TGA analyses, whose results are reported in Table III.1. As it can be seen, compared to the neat resins, DSC revealed a slight increase in the T_g values of the thermoplastic CP-based hybrids, whereas thermogravimetric analyses (TGA) showed a marked rise in the starting degradation temperature (DT_s) of all nanocomposite films. All these changes demonstrated that the addition of the organoclay, even at very low percentages, significantly improves the thermal stability of the two polymeric matrices.

Table III.1 *Glass transition temperature (T_g) and starting degradation temperature (DT_s) of neat and nanocomposite film samples.*

Organoclay amount [%]	CP-based systems		AS-based systems	
	T_g [°C]	DT_s [°C]	T_g [°C]	DT_s [°C]
0	26	327	*n.d.*	334
2	30	341	*n.d.*	365
4	29	350	*n.d.*	371
6	29	362	*n.d.*	379

III.2 Treated concrete samples characterization

In order to obtain information about the effect of the nanocomposite coatings on the water transmission rate of the concrete, WVT tests were performed on untreated CLS, used as control, and on all treated CLS samples. The results were reported in Figures III.3 (a), and (b).

The weight loss of water during the WVT tests for all specimens reached a plateau at around 380 h. As expected, the plain concrete samples show the higher values of WVT. Both neat polymeric resins don't seem to influence significantly the permeation of the treated samples. However, increasing the organoclay amount, it is noticeable that the WVT decreases, indicating a better barrier property for the nanocomposites.

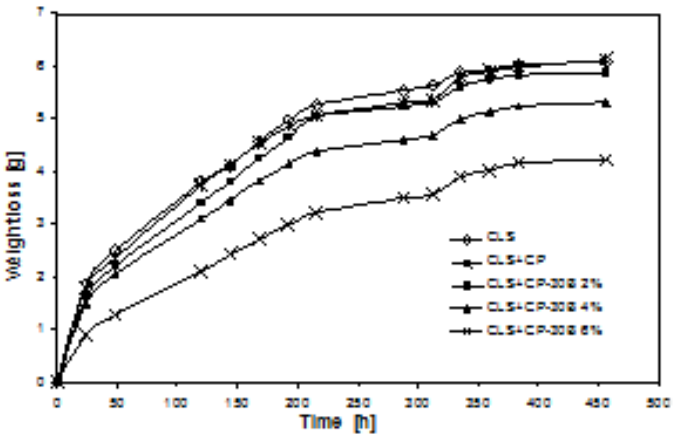

(a)

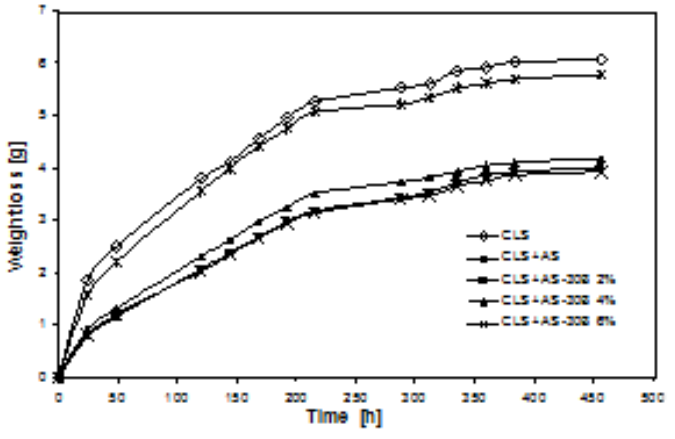

(b)

Figure III.3 *Weight loss versus time during WVT tests for concrete treated samples with Fluoline CP nanocomposites (a) and with Antipluviol S nanocomposites (b) and untreated samples.*

Similar results were already reported in literature on other organoclay-polymer nanocomposite coatings by Woo et Al. (Woo 2008), who obtained a doubling of the barrier performance of the coating by addition of 5 wt% of nanofiller.

Plotting at least six properly spaced points which are inscribed in a straight line (Figures III.4 a-b) it's possible calculate by the slope the water vapor transmission rate (WVT) and the water vapor diffusion coefficient (D_T)values and the results are shown in Figures III.5 (a-b) and in Figures III.6 (a-b). The alignment of points allow to assume that steady state is established.

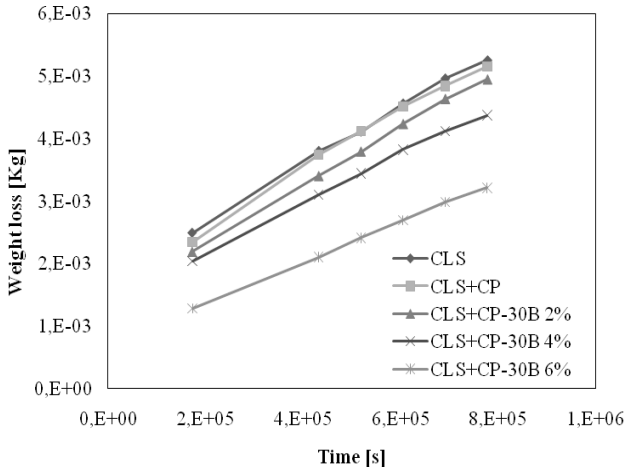

(a)

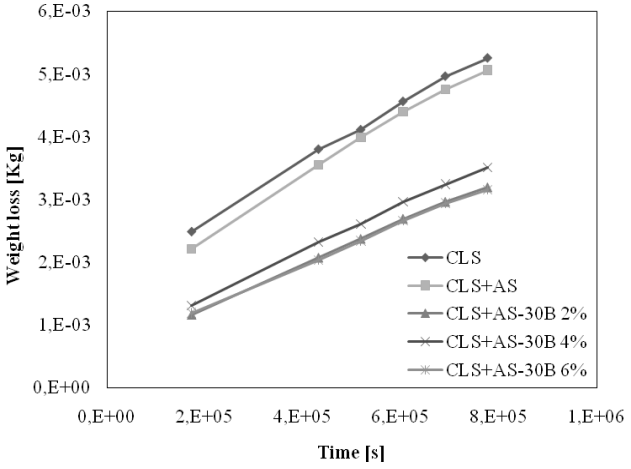

(b)

Figure III.4 *Plot of nominally steady state assumed for the calculus of WVT and DT of concrete samples dishes treated with Fluoline CP (a) and Antipluviol S (b) and their nanocomposite blends with Cloisite 30B*

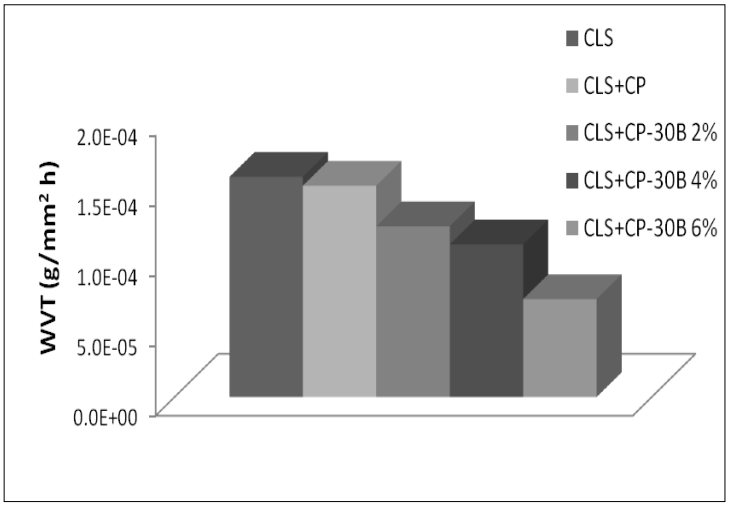

(a)

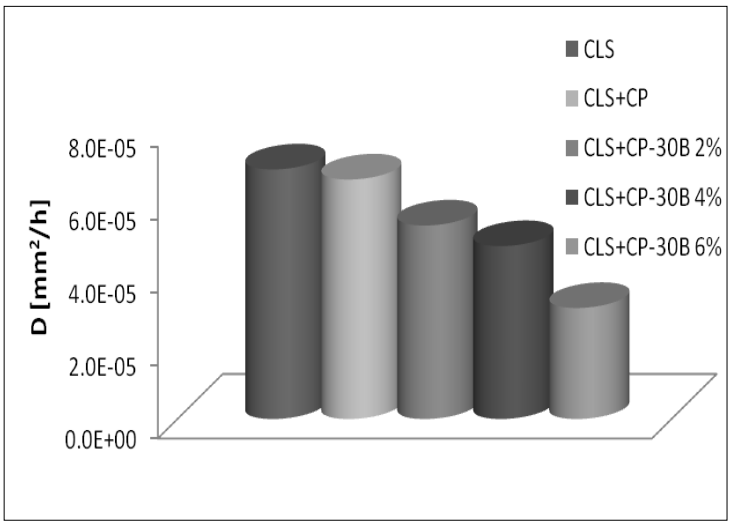

(b)

Figure III.5 *Water vapour transmission rate (a) and water vapour diffusion coefficient D_T (b) for Fluoline CP treated samples and untreated samples.*

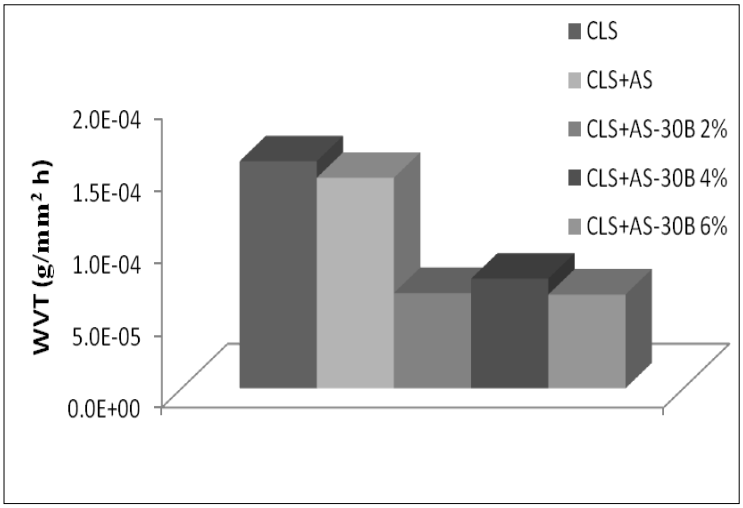

(a)

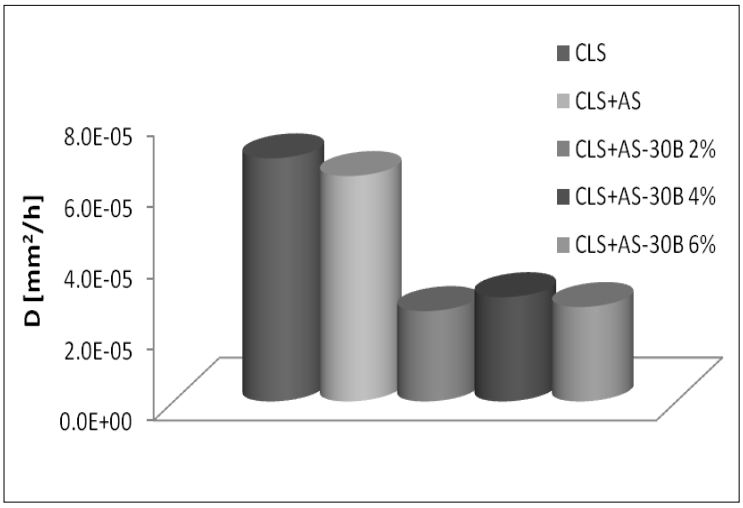

(b)

Figure III.6 *Water vapor transmission rate (a) and water vapour diffusion coefficient D_T (b) for Antipluviol S treated samples and untreated samples.*

The same test procedure has been carried out on concrete samples treated with the pore liner resin nano-loaded with Halloysite. The results were reported in Figure III.7.

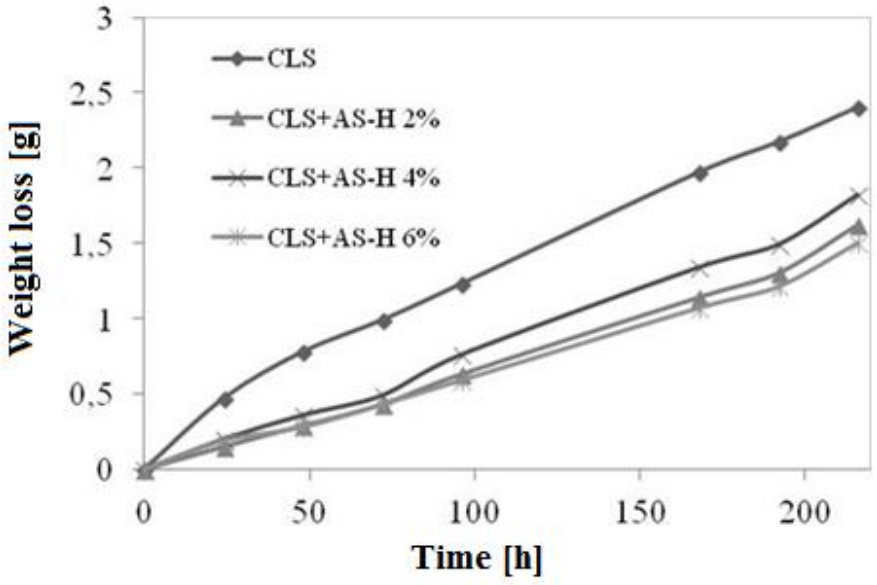

Figure III.7 *Weight loss versus time during WVT tests for concrete treated samples with Antipluviol S added with Halloysite and untreated samples.*

The numeric values of WVT of all the sample tested are reported in Table III.2.

Table III.2 *Mean values of WVT [g/h·m^2] of concrete samples treated with the nanocomposite polymeric systems.*

Sample	WVT [g/(h·m^2)]
CLS (control sample)	4.32 ± 0.17
CLS+CP	4.26 ± 0.17
CLS+CP-30B 2%	4.39 ± 0.18
CLS+CP-30B 4%	3.67 ± 0.15
CLS+CP-30B 6%	3.02 ± 0.16
CLS+AS	4.47 ± 0.19
CLS+AS-30B 2%	3.17 ± 0.17
CLS+AS-30B 4%	3.43 ± 0.18
CLS+AS-30B 6%	3.09 ± 0.16
CLS+AS-H 2%	1.29 ± 0.21
CLS+AS-H 4%	1.33 ± 0.19
CLS+AS-H 6%	1.28 ± 0.17

The results reported in Table III.2 proof that, as expected, the plain concrete samples show the higher values of WVT. On the other hand, nanocomposite systems determine a decrease of the WVT values up to about 10%, so improving the barrier properties of the resins. The results are evidently related to the high barrier properties of the lamellar and tubular clay but are also strictly dependent on its exfoliated state.

The different character of the two resins (coating or pore liner for Fluoline CP and Antipluviol S, respectively) and their chemical interaction with the two clays are most likely responsible of the extent of intercalation and exfoliation of clays within the matrixes.

These factors are correlated to the different barrier performances achieved by the three systems. In particular, the WVT reduction is quite proportional to the organoclay amount in the case of the Fluoline CP systems, whereas is almost independent from it in the case of Antipluvios S ones.

The different behavior of the three examined systems, due to the distinct character of the resins matrixes (coating and pore liner), is also highlighted by the results of capillary absorption tests.

This kind of analysis is of great significance for durability appraisement of concrete because of the fundamental role of the capillary action in the transport by which chloride and sulfate ions enter the concrete. The different character of the systems assessed in this work is evidenced by sorptivity coefficient Cw,s data reported in Table III.3.

Although both of the treatments loaded with Cloisite demonstrate the reduction of *Cw,s* , the coating (referred as CP in the table) results less effective respect to the pore liner. This is probably due to the hydrophility of clay as discussed later on.

On the other hand the pore liner (AS), which penetrates the substrate, determines a stronger hydrophobic effect within the pores in proximity to exposed surface. Moreover, the blends based on Fluoline CP show a slight reduction in the *Cw,s* values with the clay loading between 2 and 4% while Antipluviol's behavior is characterized to be not related to the clay content.

Finally a significant reduction of the sorptivity coefficient respect the control sample and the coating-based systems is evident also in the case of concrete samples treated with halloysite without any relation with the clay amount.

The difference between the two pore liner-based coating systems is due to the fact that the halloysite because of its tubular morphology is more difficult to exfoliate than the lamellar clay.

The sorptivity coefficient Cw,s data relative to the three systems are reported in Table III.3.

Table III.3 *Sorptivity coefficient (Cw,s) values of treated and untreated samples*

Samples	$C_{W,S}$ [$g/cm^2\ t^{1/2}$]
CLS	2.50 E-04
CLS+CP	1.60 E-04
CLS+CP-30B 2%	0.92 E-04
CLS+CP-30B 4%	0.88 E-04
CLS+CP-30B 6%	1.04 E-04
CLS+AS	1.20 E-04
CLS+AS-30B 2%	0.84 E-04
CLS+AS-30B 4%	0.80 E-04
CLS+AS-30B 6%	0.86 E-04
CLS+AS-H 2%	1.87E-04
CLS+AS-H 4%	1.23E-04
CLS+AS-H 6%	1.65E-04

The results of sulphate attack tests can be related to capillary behavior, since this is the most involved phenomenon in the sulphates transport thru the substrate. Figure III.8 presents the mass losses at the end of eight cycles of the sulphate attack tests. The coatings increased the protection against sulphate attack and also in this case the positive effect of nanoclay content on the protective action of resins was confirmed. The different behavior of the two kind of resins is highlighted, with better performances of the pore liner (Antipluviol S). Moreover, the nanocomposite blends have sensibly increased the protection to the attack with a minor difference between the two systems. In particular, a proportional effect of nanoclay content for the Fluoline CP based nanocomposites is noticeable, (Figure III.8) which show the best performance with the 6 wt% amount of organoclay, while optimal clay load for Antipluviol S has occurred for 4 wt% of organoclay.

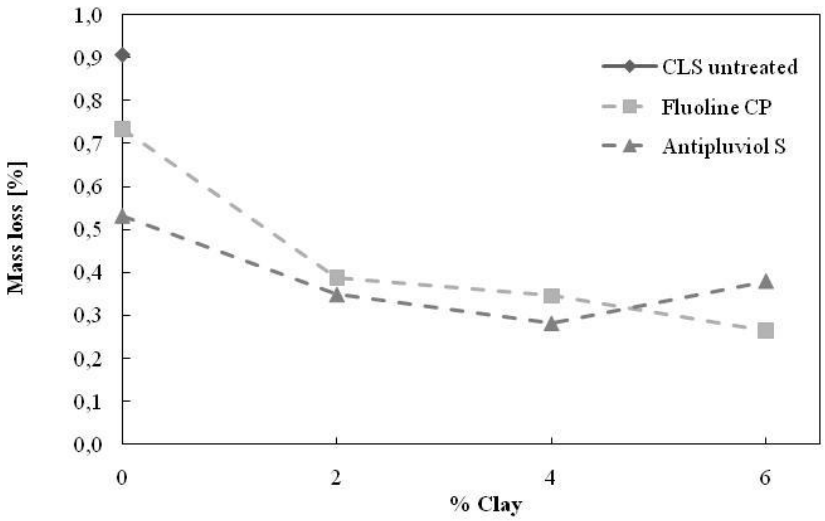

Figure III.8 *Mass loss during sulphate attack tests as a function of Cloisite30B content.*

The increasing of protection may be attributed to the efficiency of the polymeric nanocomposite resins in reducing the porosity of the concrete substrate. Tests on porosity of samples are discussed later on.

As above stated porous materials such as concrete absorb liquids mainly by capillary forces. Thus, a basic feature which characterizes the action of surface treatments for concrete is represented by their hydrophobic character which can be determined by measuring the angle of contact of water (Medeiros 2008). The values of the static contact angle, measured on the concrete surfaces coated with the different protective systems, are reported in Table III.4. In Figure III.9 the results are reported as a function of the clay concentration in the nanocomposite systems in order to evidence the trend.

The data clearly evidence that all protective treatments were effective in increasing the hydrophobic character of the rough concrete surfaces and reducing the soaking effect of water. The effect is more pronounced for samples treated with the blends containing the Antipluviol S. However, as shown in Figure III.9, the effect of clay concentration is relatively detrimental since the contact angle values slightly decrease with the organoclay content in the nanocomposite treatments. In particular, this effect is stronger for the systems based on the coating (CP) respect to the pore liner resin (AS).

These results look consistent with the values of the capillary sorption coefficient (Table III.3) which has emerged to be higher in the case of treatments based on the coating based systems (CP), with the same nanofiller.

The better performance of pore liner respect coating nanocomposite systems can be explained by considering that the pore liner can deeply penetrate into the concrete whereas the coating remains as a thin film on the surface. In this case a higher incidence of clay with its hydrophilic character is obtained on the treated surface which leads the decreasing of the contact angle (Woo 2008).

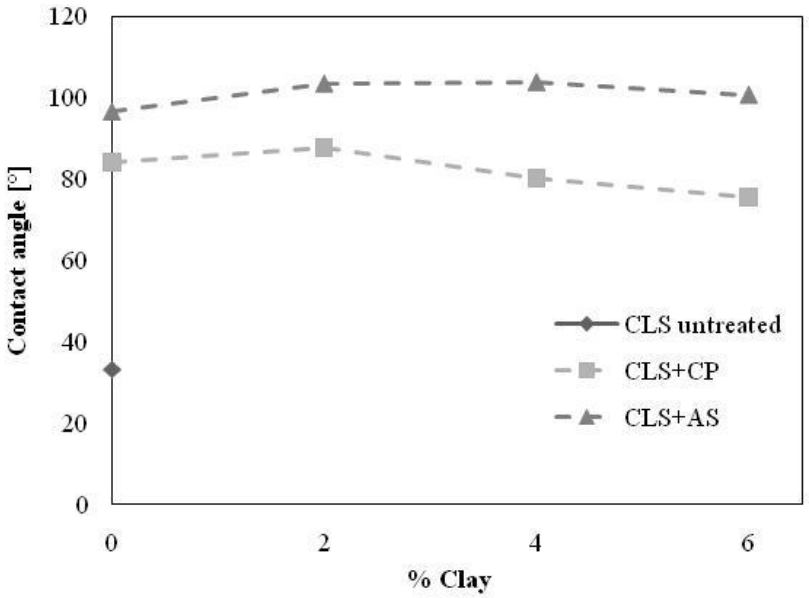

Figure III.9 *Contact angle of concrete as a function of clay loading of surface treatments.*

Table III.4 *Mean values of contact angle [°] of untreated and treated samples*

Samples	Contact angle [°]
CLS	33.2
CLS+CP	80.4
CLS+CP-30B 2%	80.6
CLS+CP-30B 4%	74.8
CLS+CP-30B 6%	71.6
CLS+AS	94.1
CLS+AS-30B 2%	103.4
CLS+AS-30B 4%	101.9
CLS+AS-30B 6%	100.6

In Figure III.10, as an example, are reported the photographs of water droplets on the surfaces of concrete samples untreated (a) and treated with

the two nanocomposite resins at 4% clay loading (b and c), taken immediately after dispensing the droplets on the concrete surfaces.

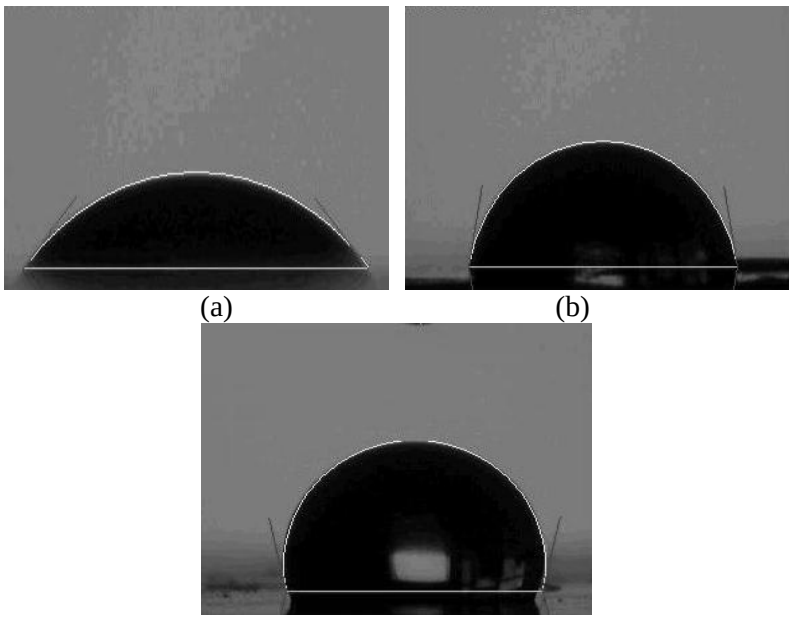

Figure III.10 *Photographs of single droplet on concrete surfaces: (a) untreated sample, (b) treated sample with Fluoline CP loaded with 2 wt% Cloisite 30B and (c) treated sample with Antipluviol S loaded with 2 wt% Cloisite 30B*

As previously stated the final performance of the treated concrete sample can be significantly affected by the different character of the two polymeric resins chosen for this work. In particular the SEM micrographs reported in Figure III.11 confirm and highlight the coating and the pore liner behavior respectively of Fluoline CP and Antipluviol S resins.

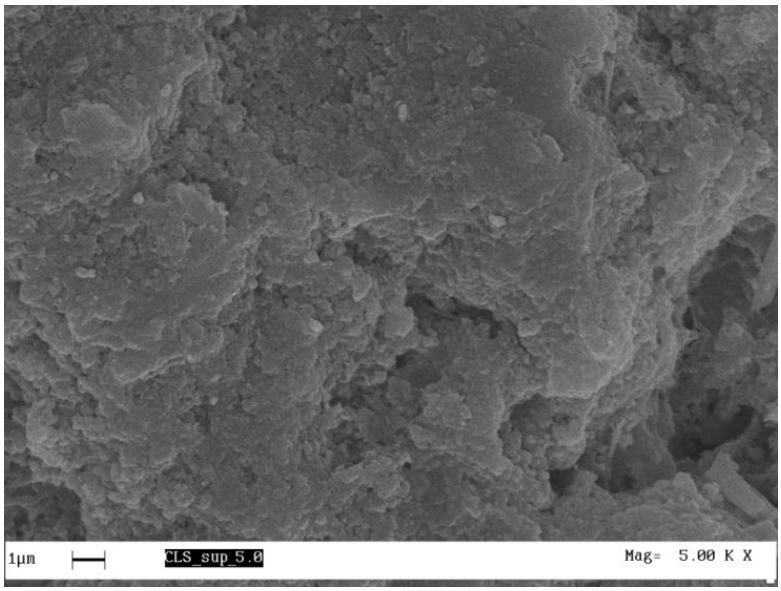

(a)

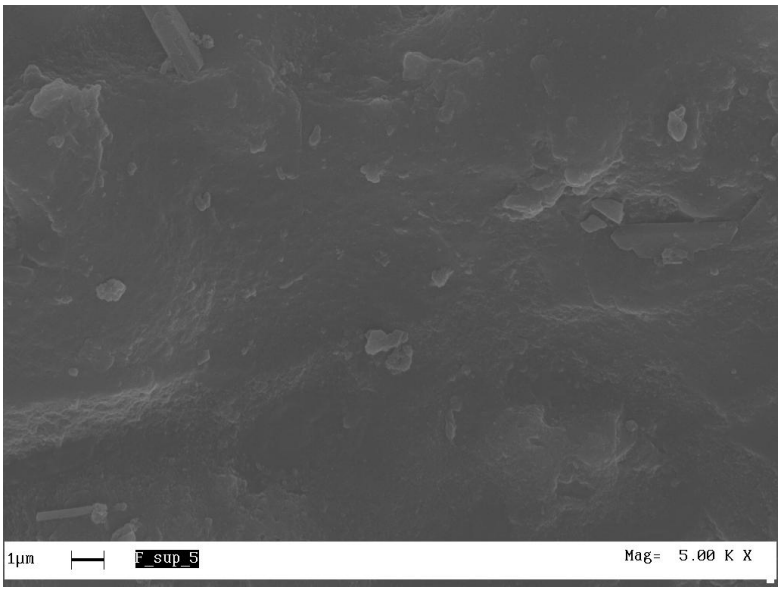

(b)

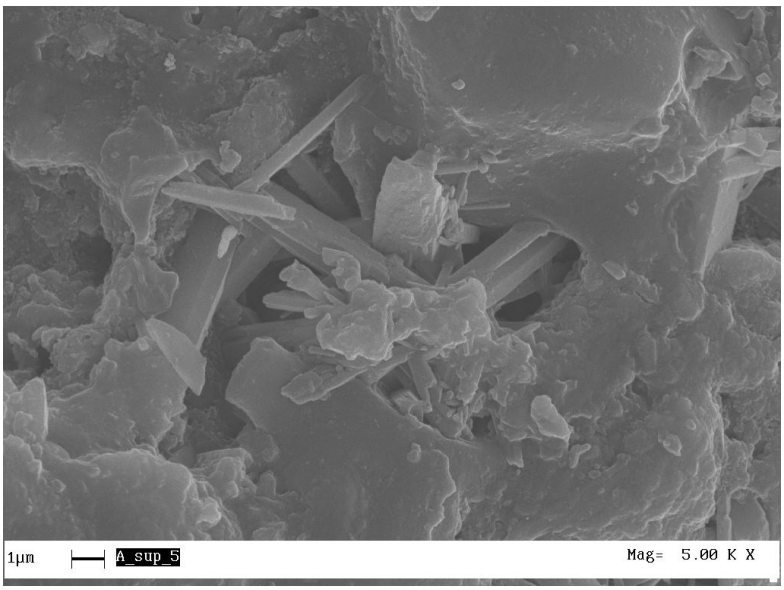

(c)

Figure III.11 *SEM micrographs on concrete surfaces: (a) untreated sample, (b) treated sample with Fluoline CP and (c) treated sample with Antipluviol S.*

As it's possible to note, while the coating remains as a thin film on the surface covering entirely the roughness of the concrete sample, the pore liner can deeply penetrate into the concrete and cover the inside walls of pores.

The different behavior of the treatments can modify considerably the porosity of the concrete substrate and thus influence the increasing of barrier performance. In order to evaluate quantitatively the porosity modification, mercury intrusion porosimetry tests were carried out on the plane concrete sample, on concrete samples treated with neat resins and with the nanocomposite systems (loaded at 4 and 6%wt of nanoclay) which have shown the more significant barrier effect in the previous tests.

Results of mercury intrusion porosimetry are reported in Figure III.12 in terms of cumulative intruded volume of Hg as function of pressure and of pore size distribution of concrete samples (Figures III.13 a-g).

Figure III.12 shows for initial concrete larger intruded volumes of Hg with respect to the treated samples and, correspondingly, a porosity of about 19.9%. The treatment with the pore liner resin (Antipluviol S) reduces the porosity of initial concrete of about 10% (sample porosity =17.7%), while the treatment of CLS with the coating resin (Fluoline CP) determines a higher decrease in porosity up to a value of 11.0%. Moreover, the addition of clay with a percentage of 4%wt decreases further the porosity for both CLS samples treated with the pore liner and the coating for which a porosity of

8.3 and 8.7%, respectively, was measured. While 6%wt of clay reduce of about half the porosity of the sample CLS+AS (4.4%) and only slightly that of CLS+CP (7.8%). These results are in accordance with the characteristic behavior of the two resins: initially the pore liner resin seems to have a small effect on porosity modification since entering inside the pores it leaves the concrete surface uncovered, while the coating resin forming a thin layer on the surface reduce drastically the porosity of the system. Adding the nanoclays while in the coating based systems the nanometric lamellas lay on surface reducing only slightly the porosity, in the case of pore liner based systems the lamellas since their nanometric dimensions are able to penetrate deep inside the pore structure.

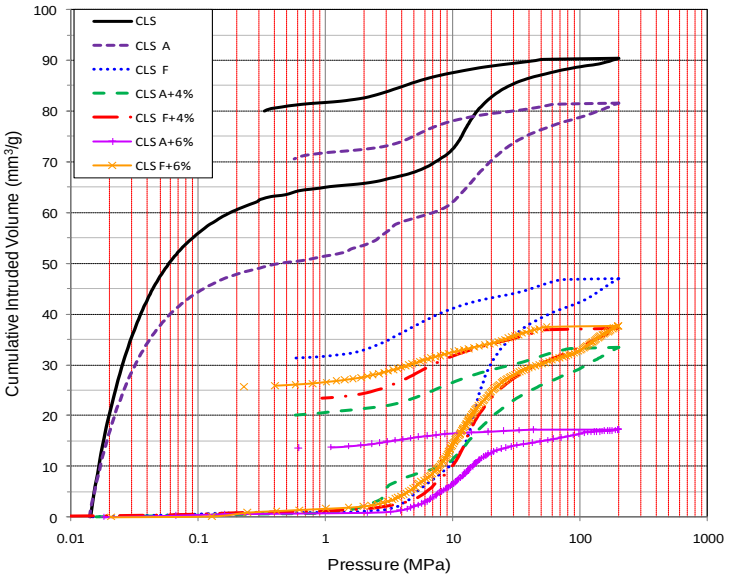

Figure III.12 *Cumulative pore volume of treated and untreated samples.*

In the following Table III.5 are summarized the results of porosity of sample analyzed.

Table III.5 *Porosity (%) of untreated and treated samples.*

Sample	Porosity (%)
CLS	19.9
CLS+AS	17.7
CLS+CP	11.0
CLS+AS-30B 4%	8.3
CLS+CP-30B 4%	8.7
CLS+AS-30B 6%	4.4
CLS+CP-30B 6%	7.8

With respect to pore size distribution the CLS has a bimodal distribution with a first peak at pore diameter of about 0.1 μm and a second peak at values ≥100μm (Figure III.13 a). The addition of Antipluviol S affects the pore structure of CLS reducing the percentage of larger pores (pore diameter in the range 10-100μm) and increasing that of pores in the range 0.4-1μm (Figure III.13 b). On the contrary the majority of pore with size larger than 1μm are clogged as consequence of Fluoline CP treatment, hence, the pore size distribution shows just the peak at 0.1 μm (Figure III.13 c).

As a consequence the effect of clay addition is more pronounced on sample treated with pore liner resin than on sample treated with coating resin. For the first (pore liner resin) it is mainly observed a reduction in larger pores (pore diameter in the range 10-100μm) with an increase in pores with diameter of about 0.5 μm when 4%wt clay is added or with diameter of 0.1-0.3 μm for 6%wt clay addition. On the contrary for the coating resin the pore distribution seems not greatly affected by the presence of clay except for the percentage of pores with 0.1 μm diameter which decreases as the clay content increases from 4 to 6%wt.

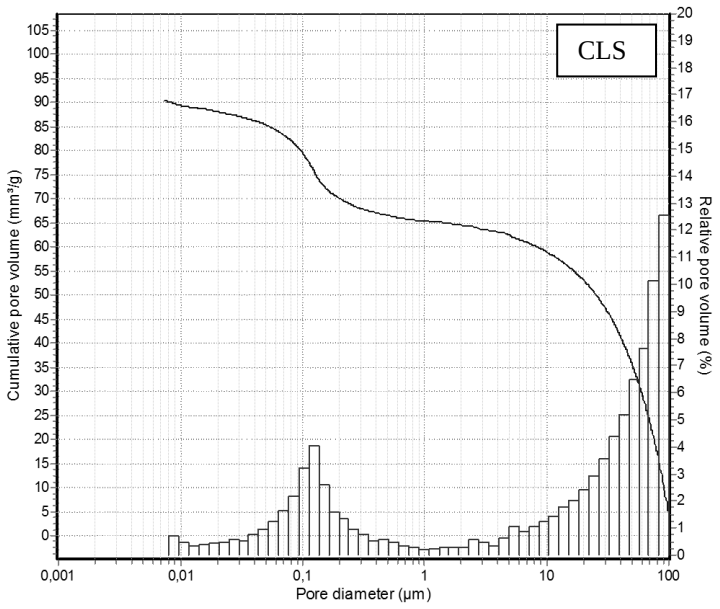

(a)

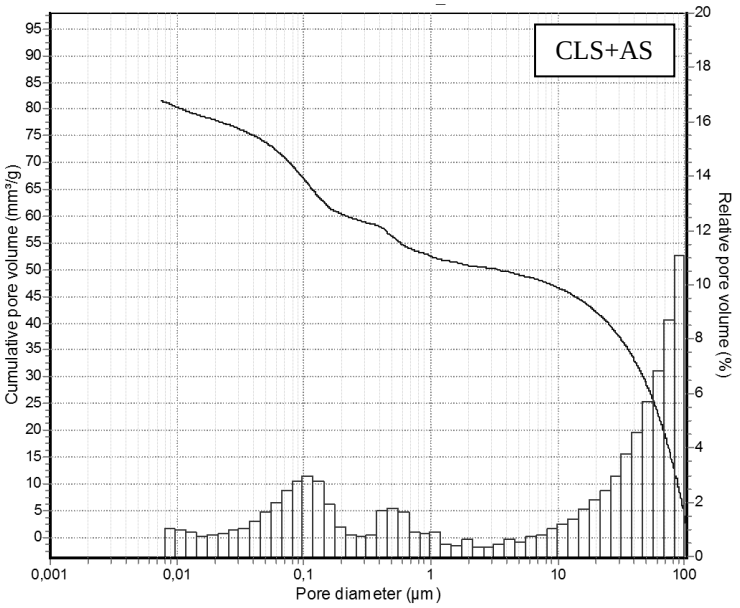
CLS+AS
Cumulative pore volume (mm³/g)
Relative pore volume (%)
Pore diameter (µm)
0,001
0,01
0,1
1
10
100

(b)

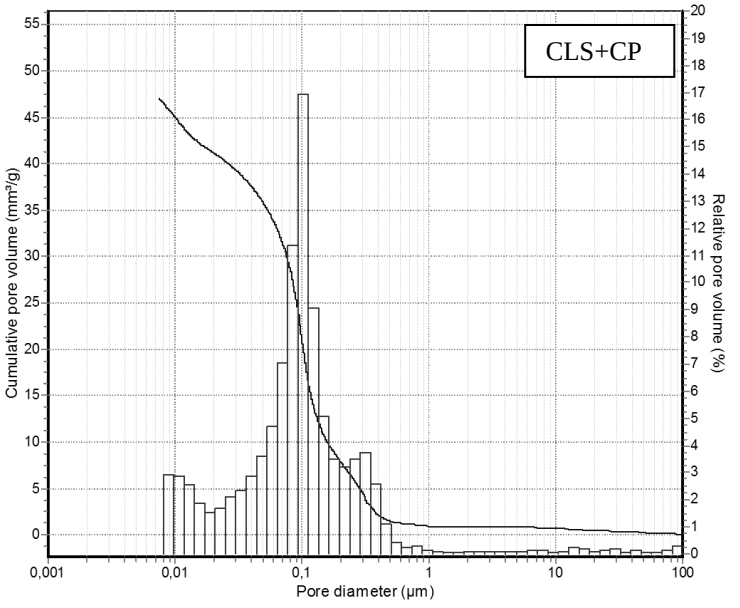
CLS+CP
Cumulative pore volume (mm³/g)
Relative pore volume (%)
Pore diameter (µm)
0,001
0,01
0,1
1
10
100

(c)

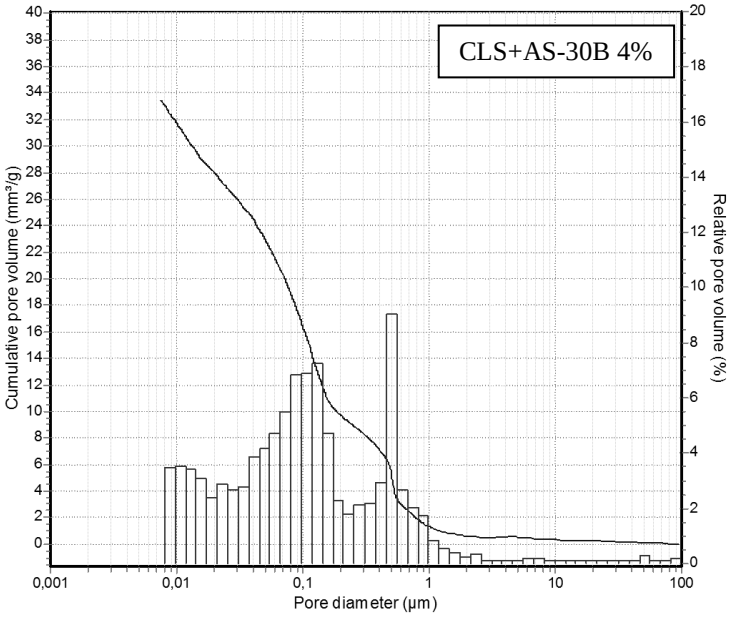
CLS+AS-30B 4%
Cumulative pore volume (mm³/g)
Relative pore volume (%)
Pore diameter (µm)
0,001
0,01
0,1
1
10
100

(d)

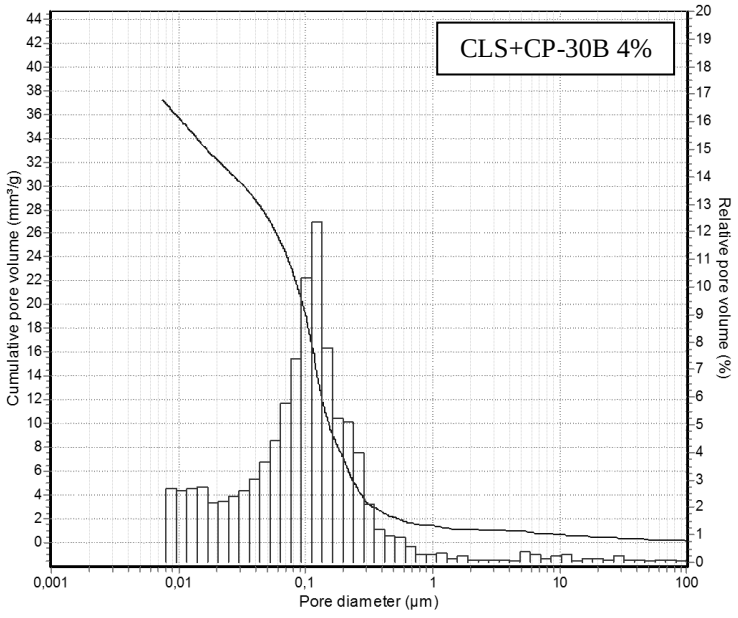
CLS+CP-30B 4%
Cumulative pore volume (mm³/g)
Relative pore volume (%)
Pore diameter (µm)
0,001
0,01
0,1
1
10
100

(e)

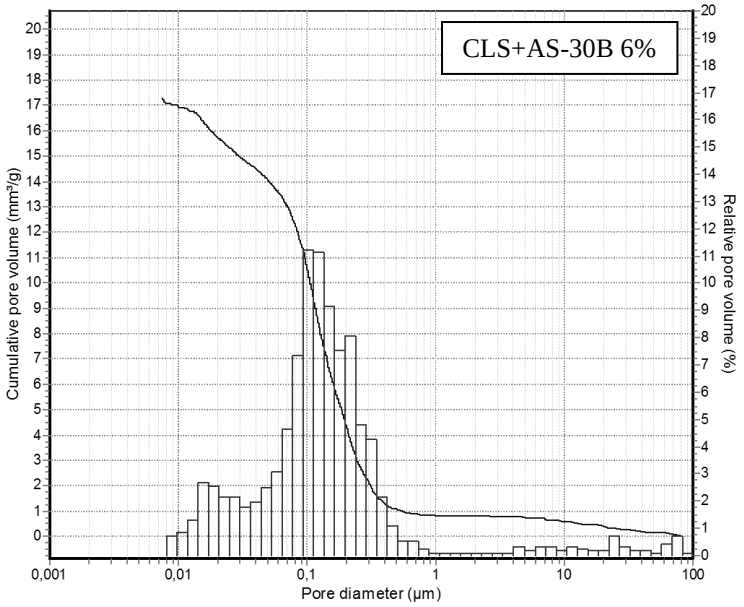

(f)

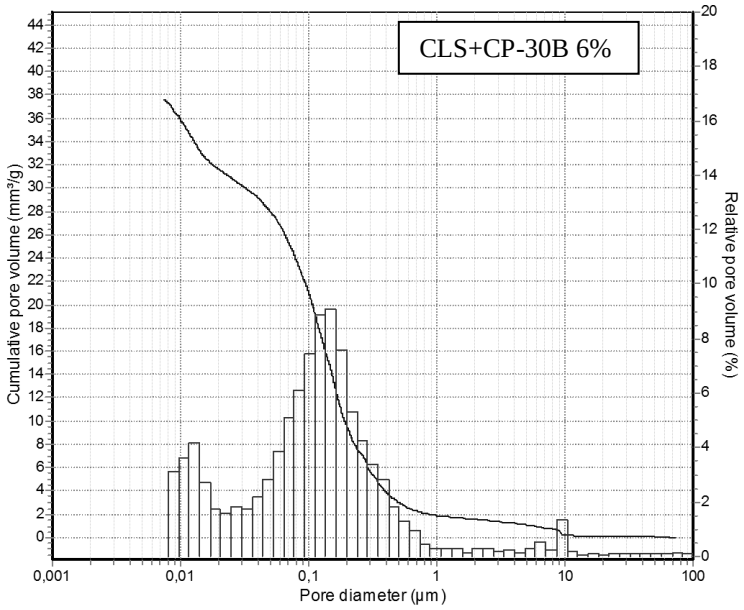

(g)

Figure III.13 *Pore size distribution of samples: (a) CLS, (b) CLS+AS, (c) CLS+CP, (d) CLS+AS-30B 4%, (e) CLS+CP-30B 4%, (f) CLS+AS-30B 6% (g) CLS+CP-30B 6%*

Finally, the aesthetic alteration of the treated concrete samples was analyzed by means of colorimetric measurements. The obtained resalts are reported in Table III.6.

Table III.6 *Color variation of concrete surface after treatments with polymeric systems*

Samples	ΔL*	Δa*	Δb*
CLS	0	0	0
CLS+CP	-1.63	0.07	0.09
CLS+CP-30B 2%	-1.44	0.06	0.07
CLS+CP-30B 4%	-0.88	0.02	-0.13
CLS+CP-30B 6%	-0.44	0.05	-0.05
CLS+AS	-4.25	0.16	0.89
CLS+AS-30B 2%	-4.03	0.18	0.59
CLS+AS-30B 4%	-3.96	0.11	0.63
CLS+AS-30B 6%	-3.48	0.13	0.56

After the application the alteration in the appearance of the treated concrete surface results in a modest variation of the brightness differences ΔL*. On the other hand, the values of a* (chromatic parameter towards the red) and b* (chromatic parameter from blue to yellow) appear not or slightly affected by the treatments with the polymeric resins and are not related to clay content.

III.3 UV weathering of surface treatments

In a preliminary study, have been evaluated also the protective efficacy and stability of polymeric nanocomposites for concrete (CLS) surface protection against UV weathering.

As previously discussed, DSC and TGA analyses have demonstrated that the addition of the organoclay, even at very low percentages, significantly improves the thermal stability of the two polymeric matrices.

In order to verify if similar beneficial effects occur towards UV radiation weathering, too, all film samples were exposed for 7 day to UV light in a climatic chamber and their colorimetric variations and FT-IR spectra were measured and compared with that recorded on the unweathered specimens. As for example, in Table III.7 are reported the colorimetric results obtained on samples unloaded and loaded with 4wt% of organoclay, whereas in Figure III.14 are shown the corresponding FT-IR spectra.

Table III.7 *Colorimetric variations of polymeric films after UV exposure.*

Film samples	Unaged films				Films aged for 7 days under UV light			
	ΔL*	Δa*	Δb*	$\Delta E_{a,b}$	ΔL*	Δa*	Δb*	$\Delta E_{a,b}$
CP	--	--	--	--	-0.5	0.13	0.2	0.55
CP-30B 4%	-1.5	-0.25	2.0	2.51	-0.7	-0.86	0.3	1.15
AS	--	--	--	--	-1.2	-0.31	0.4	1.30
AS-30B 4%	-0.3	-0.19	0.8	0.88	-0.8	-1.55	0.5	1.81

The data of Table 11 evidences that the color changes, measured as a difference in brightness value (L*) and a* and b* coordinates, and the chromatic differences $\Delta E_{a,b}$ before and after UV light exposure are in all cases very small, undetectable to naked eye. Anyway, FT-IR measurements showed that while the Antipluviol S films based, both neat and nanocomposite, don't seem to be sensible to the degradative effects, the neat Fluoline CP film based shows a marked increase in intensity of the peak corresponding to the presence of carbonyl groups, suggesting that the photo-oxidation phenomena has occurred. However, at the same UV exposure time, the CP-based nanocomposite film shows the intensity of the peak in correspondence of carbonyl groups significantly reduced. The ATR FT-IR spectra, recorded before and after the exposure of the samples to UV light for 7 days (Figure III.14), showed that the increase in the intensity of the carbonyl signal is significantly lower for the hybrid than for the neat resin suggesting that organoclay presence reduce sensibly the photo-oxidation phenomena due to UV exposure.

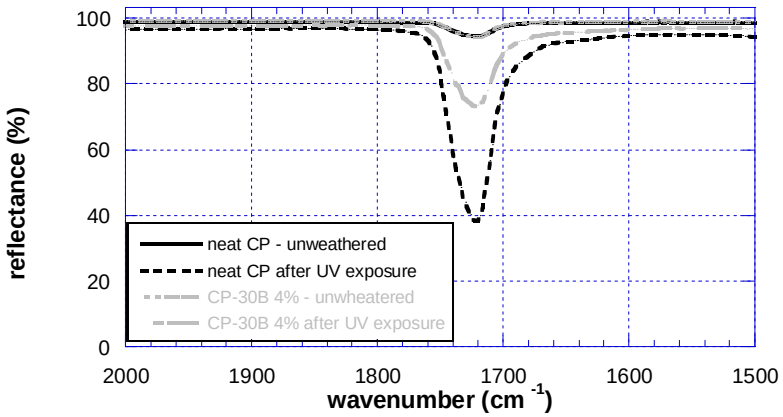

Figure III.14 *ATR FT-IR spectra of CP-based nanocomposite films at different composition, before and after UV exposure.*

Chapter IV
Results of hydrophobic-nanocomposite concrete characterizations

In light of the results shown in the previous chapter, which evidenced a better performance for the pore liner based nanocomposite systems, it has been decided to proceed using the same polymer matrix based on silane-siloxane, this time in aqueous solution, and the same nanoclay in the concrete mix in order respectively to make the whole system hydrophobic, and to modify the microstructure of cement paste.

IV.1 Cloisite modified hydrophobic concrete

Since water is considered the principal cause of degradation of concrete structure, because it acts as vehicle for the aggressive substance, water inlet capacity for all the samples produced has been studied through capillary adsorption test and water immersion test in atmosphere and under vacuum.

In Figure IV.1 is reported the water capillary adsorption of all samples as a function of time. Nanocomposite samples and even more the hydrophobic samples reduce their capacity to absorb water by capillary action than the control sample. The nanoclay modify internal microstructure of mortars obstructing the pore cavities, moreover the montmorillonite modified by a cationic-exchange reaction becomes hydrophobic and most probably it can prevent water passing between silicate sheets. On the other hand, as we expected, the hydrophobic agent used as admixture additive lowers very significantly the molecular attraction between water and the concrete pore walls reducing water rising by capillary of about 70%. The Figure IV.1 highlights also another important difference between the nanocomposite and hydrophobic mortar samples in reaching the saturation time: longer for the second ones. In Table IV.1 are reported the sorptivity coefficients of the samples.

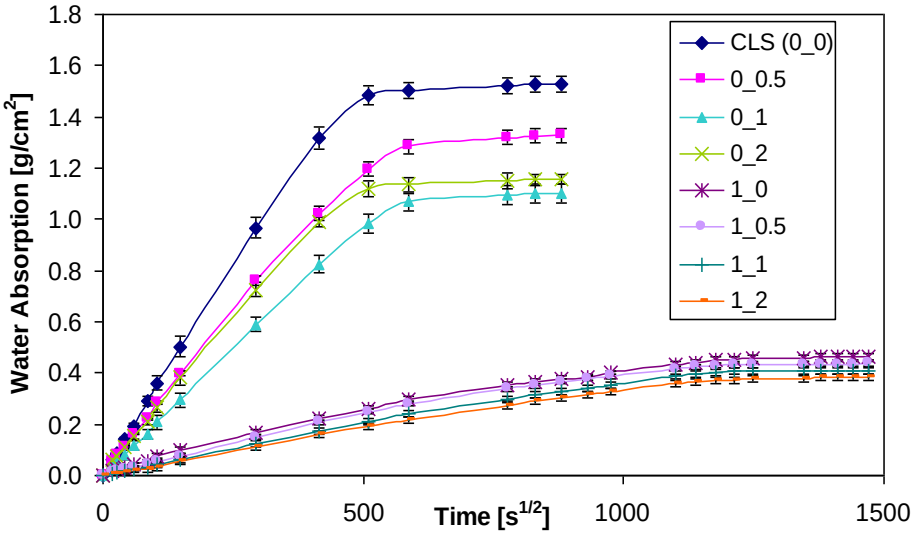

Figure IV.1 *Capillary absorption profiles of concrete samples modified by adding of hydrophobic resin and Cloisite 30B*

Table IV.1 *Sorptivity coefficient (Cw,s) values of reference sample and modified concrete samples*

Samples	$C_{W,S}$ [g/cm^2/t$^{1/2}$]
CLS	3.48E-03
0_0.5	2.70E-03
0_1	2.01E-03
0_2	2.59E-03
1_0	6.78E-04
1_0.5	5.02E-04
1_1	3.78E-04
1_2	2.91E-04

In the water immersion test carried out in atmosphere the hydrophobic resin more efficiently reduces the water absorption, while the clay content does not seem to affect it. By the water immersion under vacuum test, instead, the role of clay in modification of microstructure, closing the pore structure, is more noticeable (Figure IV.2).

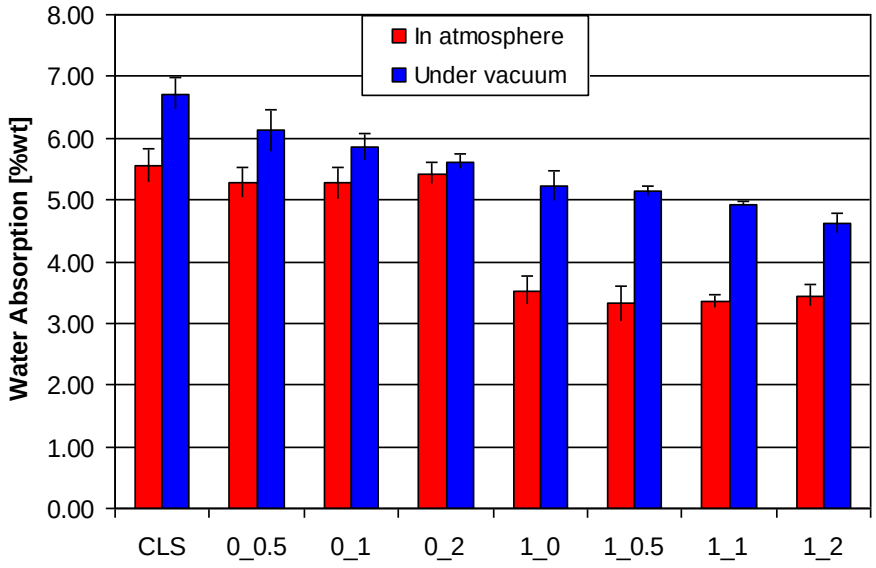

Figure IV.2 *Water Absorption of concrete sample modified by adding of hydrophobic resin and Cloisite 30B*

In Table IV.2 are reported the water absorption values in percentage in weight for all the samples tested in atmosphere and under vacuum.

Table IV.2 *Water Absorption values in atmosphere and under vacuum*

Samples	Water Adsorption [%]	Water Adsorption under vacuum [%]
CLS (0_0)	5.54 ± 0.27	6.71 ± 0.26
0_0.5	5.28 ± 0.24	6.12 ± 0.33
0_1	5.27 ± 0.27	5.85 ± 0.22
0_2	5.43 ± 0.18	5.62 ± 0.12
1_0	3.53 ± 0.23	5.23 ± 0.25
1_0.5	3.32 ± 0.30	5.13 ± 0.08
1_1	3.36 ± 0.18	4.93 ± 0.04
1_2	3.44 ± 0.11	4.62 ± 0.15

Through the water absorption test by immersion has also been investigated the open and accessible porosity of all the samples. Open porosity is defined as the ratio between specific volume and water absorption, and accessible porosity as the ratio between specific volume and water absorption under vacuum (Courard 2003). In Table IV.3 are reported the calculated values of open and accessible porosity.

Table IV.3 *Open and Accessible porosity of concrete sample modified by adding of hydrophobic resin and Cloisite 30B*

Samples	Open porosity [% vol]	Accessible porosity [% vol]
CLS (0_0)	12.61 ± 0.42	15.24 ± 0.31
0_0.5	12.12 ± 0.28	14.08 ± 0.18
0_1	12.14 ± 0.31	13.50 ± 0.22
0_2	12.22 ± 0.12	13.22 ± 0.27
1_0	7.22 ± 0.18	13.05 ± 0.19
1_0.5	7.69 ± 0.22	12.13 ± 0.21
1_1	6.86 ± 0.19	11.47 ± 0.09
1_2	7.52 ± 0.25	10.65 ± 0.31

In order to evaluate the effectiveness of the nanocomposite and hydrophobic additives, all the systems of concrete specimens were tested by chloride diffusion test. The incorporation of nanoclay (Figure IV.3) in the mortars improved their chloride penetration resistance. Anyway, clay amount don't seem have any significative effect.

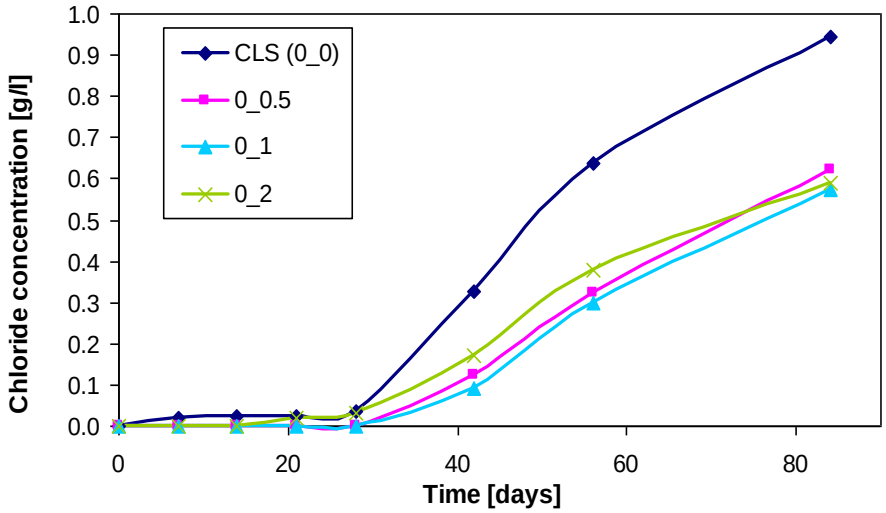

Figure IV.3 *Chloride concentration versus time of control and nanocomposite mortar samples*

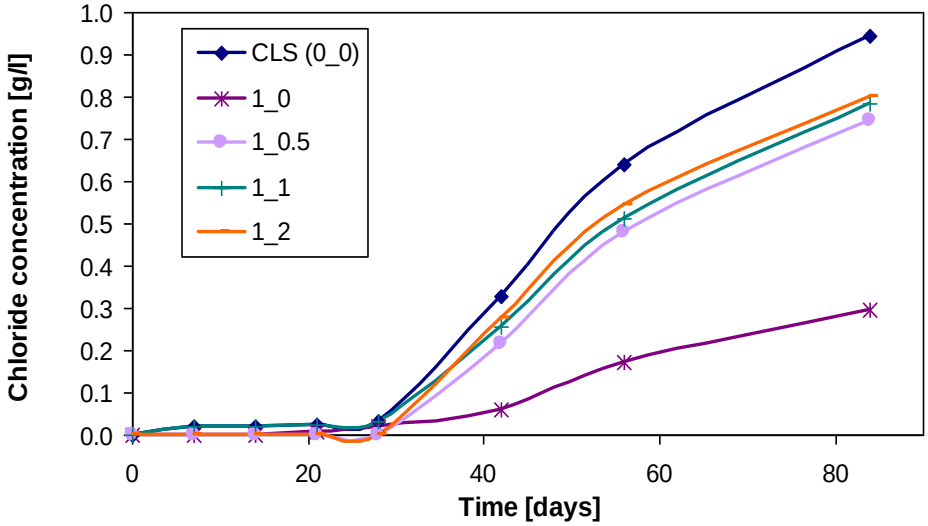

Figure IV.4 *Chloride concentration versus time of control and hydrophobic mortars nanoloaded and not.*

The solely hydrophobic agent in concrete causes the reduction of the chloride diffusion (Figure IV.4), but in presence of nanoclay this positive effect is strongly reduced. Which is the reason of this apparently strange behavior? To better understand the interaction between the system polymer-nanoclay with chloride ions ATR/FT-IR Analysis are carried out on the nanoclay as it is and on nanoclay immersed in a chloride ions saturated solution and the spectra FT-IR are reported in Figure IV.5.

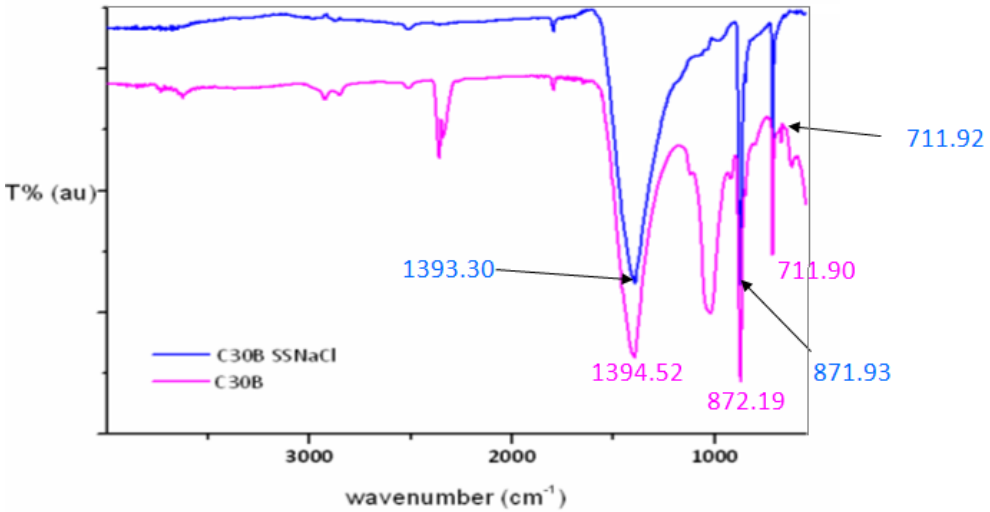

Figure IV.5 *FT-IR Analysis of neat nanoclay and on nanoclay immersed in chloride solution*

From the chemical point of view we can see by the FT-IR Analysis that the nanoclay in presence of saturated solution of sodium chloride doesn't have any chemical structure modification. So probably the interaction is related to an aspect of physical type: the silica lamellae dispersed in the hydrophobic resin may create some discontinuity in the continuous film covering the inside wall pores letting the ions chloride diffusion more easy.

Regarding the following gas diffusion study, we are expected that the hydrophobic resin into modified concrete doesn't have any important effect because it acts especially as protective for liquid, of course, but in this paper the hydrophobic samples are in any case investigated because we are interested in study the efficacy of the nanoclay with and without the presence of a hydrophobic resin.

The resistance to carbonation can be measured by the depth of carbonation determined using a color indicator, the phenolphthaline. In Figure IV.6 is reported the evolution of the depth of carbonation over time. The results show an improvement in carbonation resistance for all the nanocomposite hydrophobic or non hydrophobic samples, while in the case of the hydrophobic sample without adding of nanoclay (1_0) the carbonation resistance gets worse. As confirmed in the literature, with the addition of the polymer, the rate of carbonation of the hardened pastes was increased despite the decrease in their water absorption (Aimin 1988). The nanoclay added to the cementitious matrix improves the carbonation resistance and this action is not related or is slightly related to the amount of nanoclay and doesn't seem to be influenced by the presence of the resin; instead the hydrophobic sample without nanoclay (with only the resin inside it) shows a depth of carbonation greater than all the other samples, also than the control one. This results confirm that, as said before, the presence of polymer accelerates the carbonation rate, because, due to its intrinsic nature, the hydrophobic resin makes the pores of the mortar unsatured of water and so make them empty, facilitating in this case the CO_2 passage. Adding the nanoclay this effect seems to be mitigated and the action of the nanoparticles of closing the porosity seems predominant and absolutely not affected by the presence of the hydrophobic resin.

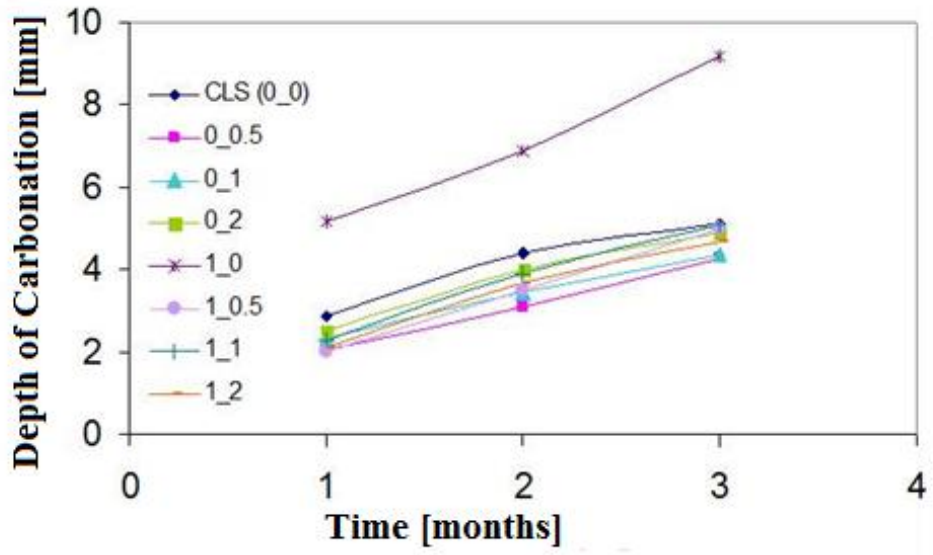

Figure IV.6 *Depth of carbonation over time*

In pictures of Figure IV.7 are shown the carbonated samples sprayed with phenolphthalein: the pink zones are indicative of not carbonation while the white zones are the parts of the samples carbonated more deeper for the sample with the solely hydrophobic resin.

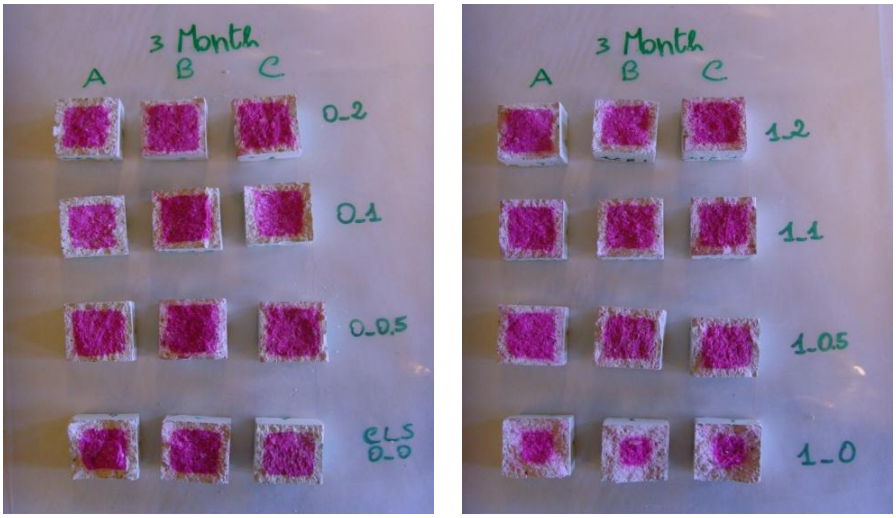

Figure IV.7 *Carbonated samples spryed with phenolphthaline*

In Figure IV.8 is the evolution of intrinsic permeability of oxygen as a function of the content of clay and in Table IV.4 the numerical values are reported.

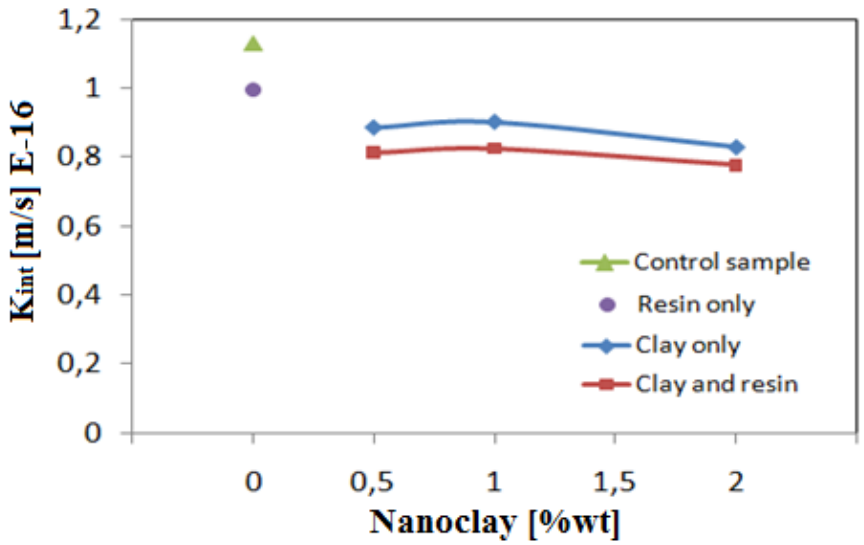

Figure IV.8 *Intrinsic Permeability of oxygen as a function of the content of clay*

Also in this case, the nanoparticles show a positive effect in reducing the gas diffusion, thanks to their obstruction action in the concrete pores, without any important difference in presence or not of the hydrophobic resin.

Regarding the only hydrophobic sample (1_0), in literature some authors state that oxygen diffusion could directly occur in a gaseous phase through the unsatured porosity of the immersed hydrophobic concrete, while in concrete without silane, oxygen diffuses much slower through water filling the pores of the saturated concrete (Tittarelli 2009). In agreement with the literature we have to expect an increase in oxygen permeability for the hydrophobic sample not nano-loaded and so this should imply a pejorative effect of the presence of the hydrophobic additive. In true the value of permeability of the sample 1_0 (that one containing the solely resin) is not very different respect the control sample, indeed it is slightly reduced, while as it's clear the nanocomposite-hydrophobic samples don't seem to be influenced by the silane-siloxane resin.

Table IV.4 *Average values of intrinsic permeability*

Samples	K_{int} [m/s]
0_0	1,13E-16
0_0.5	8,85E-17
0_1	9,01E-17
0_2	8,28E-17
1_0	9,97E-17
1_0.5	8,13E-17
1_1	8,25E-17
1_2	7,77E-17

Regarding the sulphates test at present no significant variation in length has been registered.

In order to verify the effect of the hydrophobic resin and especially of the nanoclay on modification of macro and micro-structure of cement paste the mercury intrusion porosimetry tests are carried out and the results are reported in Figure IV.9 (a, b and c) in terms of cumulative and relative intruded volume of Hg as function of pore size distribution of concrete samples. As an example, to better highlight the different effect of the two ingredients added to mix concrete, are reported the results of the white sample (or control sample) and of the 1_0 and 0_2 samples, respectively with the only hydrophobic resin (at 1%wt respect the cement) and with the only nanoclay (at 2%wt respect the cement).
CLS

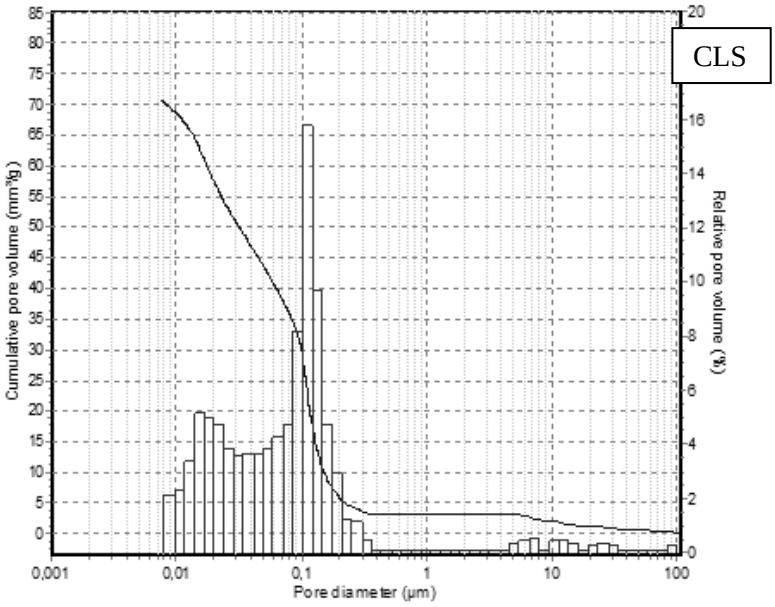
CLS
Cumulative pore volume (mm³/g)
Relative pore volume (%)
Pore diameter (µm)
0,001
0,01
0,1
1
10
100

(a)

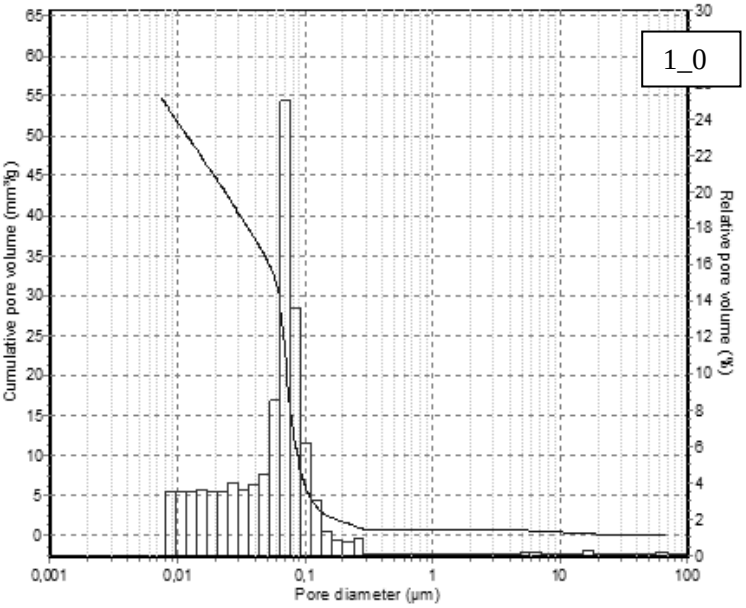
1_0
Cumulative pore volume (mm³/g)
Relative pore volume (%)
Pore diameter (µm)
0,001
0,01
0,1
1
10
100

(b)

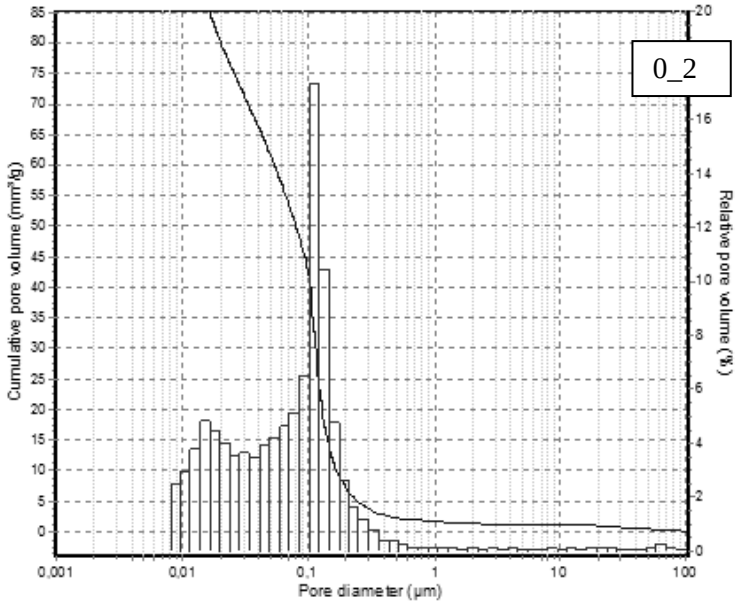

(c)

Figure IV.9 *Pore size distribution of samples: (a) CLS, (b) 1_0 and (c) 0_2*

Figure IV.9 shows for the 1_0 sample a reduction of macroporosity (from 10 to 100 µm, which is the maximum value that we can measure whit our instrument), while the sample 0_2 shows an increase of capillary pores (from 0.1 to 10 µm).

These results are in agreement with what we are expected: on one side the pore liner resin seems to have an effect only on macroporosity modification thanks to its character of water repellent which acts covering all the inside walls of pores with only a thin film and reducing the inner diameter of pores, while on the other side the nanoclays act as nuclei for cement phase, further promoting cement hydration and accelerating so the growth of the microporosity.

IV.2 Halloysite modified hydrophobic concrete

Water inlet capacity has been studied through capillary adsorption test and water immersion test in atmosphere and under vacuum, also for the concrete samples, hydrophobic and not, modified by adding of halloysite.

In Figure IV.10 are reported the water absorption by capillary profiles versus the square root of time.

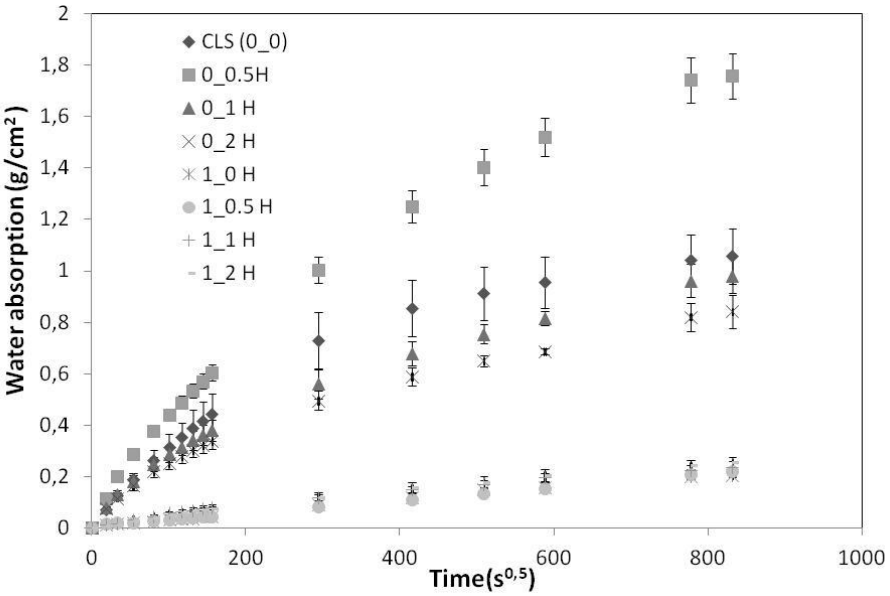

Figure IV.10 *Capillary absorption profiles of concrete samplesmodified by adding of hydrophobic resin and Halloysite*

The results reported show that at low percentage of Halloysite, seems to be predominate the hydrophilic character of the nanoparticles in question and then the water tends to seep into the pores much more than into the white sample. At higher percentage of Halloysite the water absorption decreases gradually, probably thanks to the fact that in larger amounts the Halloysite works as filler of pores by limiting the whole porosity. Finally, as we expected the introducing of Antipluviol S into the mix concrete reduce considerably the water absorption, but the different percentage of nanoparticles doesn't modify it significantly.

Regarding the water absorption in atmosphere of the same concrete samples, the results are reported in Figure IV.11.

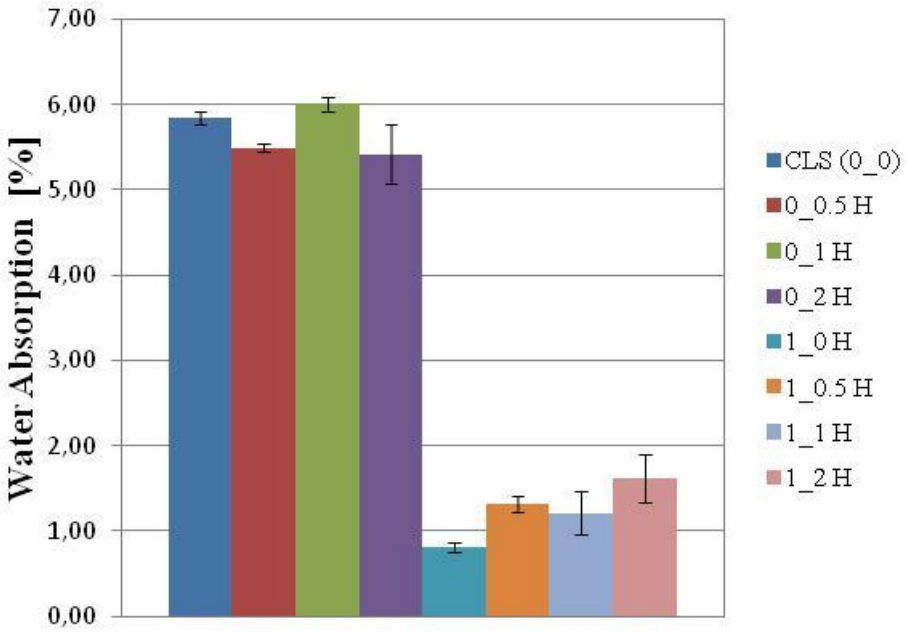

Figure IV.11 *Water Absorption of concrete sample modified by adding of hydrophobic resin and Halloysite*

We can see that the solely Halloysite doesn't seem to have any important effect on the modification of water inlet capacity, but only a slightly reduction in the cases of 0.5 and 2%wt of Halloysite amount.

Instead, a strong fall of water absorption happens with the adding of the only resin which is the better performance, in fact adding gradually the Halloysite the water absorption, even if a little, worsens.

In Table IV.5 are reported the numerical results of the open porosity.

Table IV.5 *Open porosity of concrete sample modified by adding of hydrophobic resin and Halloysite*

Samples	Open porosity [% vol]
CLS (0_0)	13.44± 0.09
0_0.5H	12.39 ± 0.23
0_1 H	13.26 ± 0.28
0_2 H	11.72 ± 0.31
1_0 H	2.42 ± 0.33
1_0.5 H	2.78 ± 0.17
1_1 H	2.58 ± 0.25
1_2 H	3.57 ± 0. 22

IV.3 Mechanical properties

IV.3.1 Dynamic Modulus of Elasticity

Ultrasonic waves can be used to determine composition, density, compressibility, temperature, elastic modulus, texture, and microstructure, as well as to locate and characterize voids or inclusions, and monitor aggregation processes (Wright 2011) and so by measuring the velocity of ultrasonic waves in relation with Poisson's ratio the dynamic modulus of elasticity is calculated (Qixian 1996).

The measurement of the propagation velocity of ultrasonic waves in the concrete samples was assessed by the method of direct transmission linked to a length of the trajectory well-defined because the probes are positioned on the opposite faces of the sample to be investigated.

The measured 3-day until 12-day dynamic modulus of elasticity of concrete samples added or not with cloisite, halloysite and the hydrophobic resin are shown in Figure IV.12 a-b.

Almost all the samples reported in the following figures in the first days of cement maturation show a decrease of elastic modulus after an initial increase, and then another ascent.

This can be explained by referring to the fact that cement materials exhibit a continuous change in the mechanical properties with time due to a chemical reaction known as hydration; there is a steady increase in the stiffness after setting (Subramaniam 2005).

In fact the calcium hydroxide, produced during hydration of the silicate has a less dense structure than aluminate hydrates which are formed during the hardening phase; gradually, then, the internal structure becomes more compact in relation to the development of secondary silicates and aluminates which are formed during the pozzolanic reaction (the silica and alumina in amorphous form, contained in the pozzolan, react with the hydroxide to form the secondary calcium silicates and aluminates hydrates) and the dynamic modulus tends to rise again.

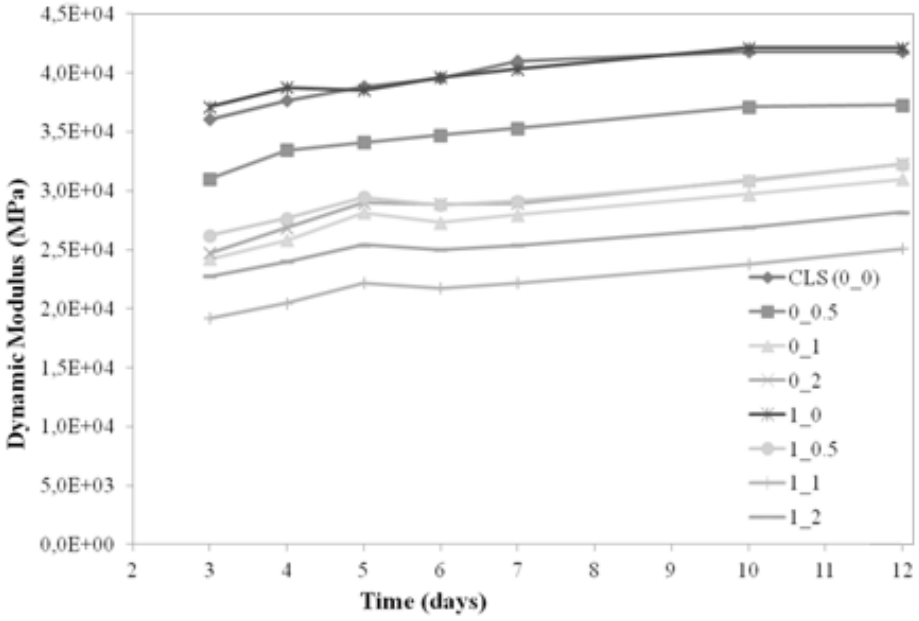

(a)

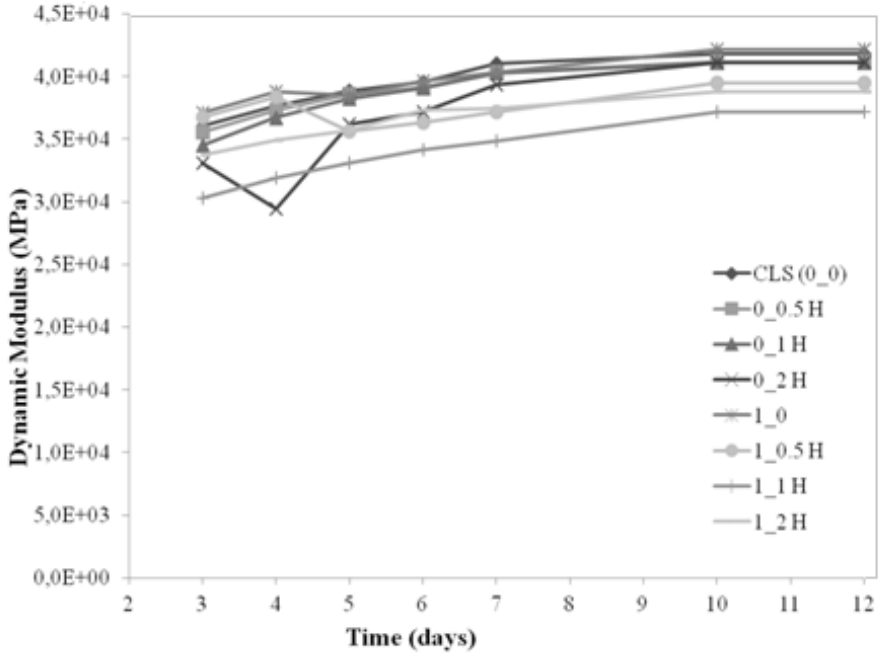

(b)

Figure IV.12 *Elastic Dynamic Modulus of concrete sample modified by adding of hydrophobic resin and Cloisite (a) or Halloysite (b).*

Moreover the use of the hydrophobic resin in the mixture does not negatively affect on the mechanical characteristics of the concrete, while the addition of halloysite and especially of cloisite seems to adversely affect it probably because the presence of nanoparticles inside the matrix could create some microvoids which means lower elastic dynamic modulus.

IV.3.2 Compressive Resistance test

In Figure IV.13 and IV.14 are reported the results of Compression Resistance test.

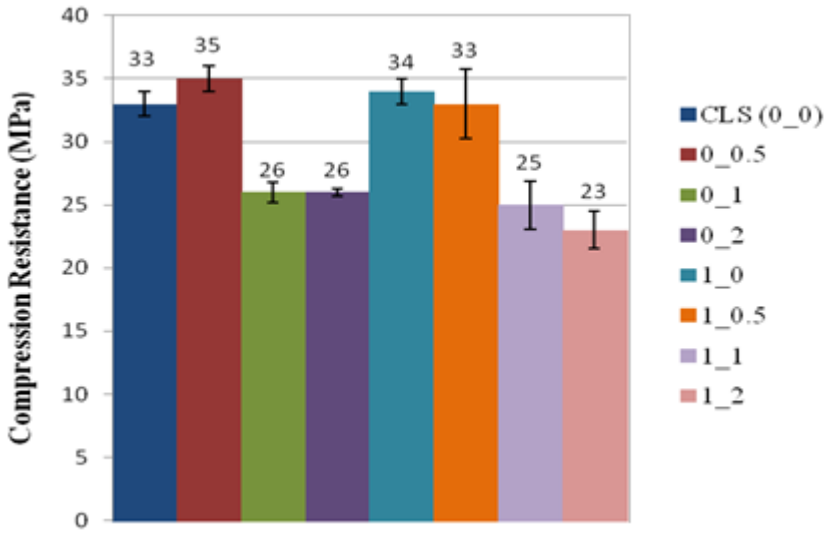

Figure IV.13 *Compression Modulus of concrete samples modified by adding of hydrophobic resin and Cloisite*

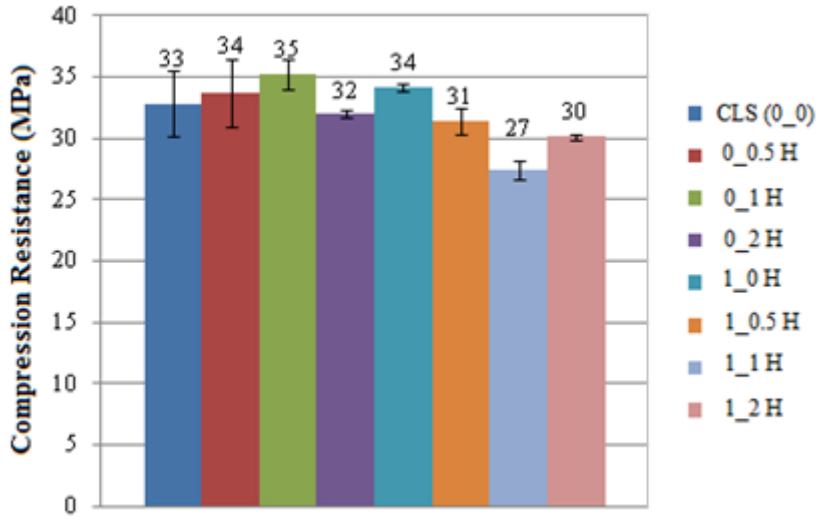

Figure IV.14 *Compression Modulus of concrete samples modified by adding of hydrophobic resin and Halloysite*

As shown in Figures IV.13 and IV.14, the additions of lamella of cloysite and of nanotubes of halloysite to the concrete mixtures does not seem to improve significantly the compression resistance of the samples, except for percentage of nanoparticles ranging between 0.5 and 1 %wt.

Similarly, the addition of the hydrophobic resin, as expected, doesn't affect the compressive strength of the samples.

As well know in literature, a good dispersion of nano-meter particles promotes the cement hydration, which means improved mechanical properties.

In fact, with ultrafine particle size reducing to nano-structured one, specific surface and the number of atoms in the surface increase rapidly (Ye 2007). For this reason, the nano-meter particles, have high surface energy and atoms in the surface have a high activity, which leads the atoms to react on outer ones easily (Zelic 2000) easing the hydration reaction.

So we can think that, in our case, at high amount of nanoparticles the dispersion doesn't occurs at nanometric level. Proper dispersion and adequate load transfer are the main challenges in the search for efficient reinforced cement composites (Musso 2009).

Nevertheless, adding cement with a high specific surface material would increase the wettable surface area and the amount of water adsorbed by the hydrophilic groups present on the two kind of montmorillonite surface.

The nanoparticles absorb a not-negligible amount of water hampering the cement paste hydration (Dweck 2002). This is the other reason why as the content of nanoparticles increases, mechanical performances worsen.

Chapter V
Theoretical fundamentals of chloride diffusion

V.1 Mass transport in the chloride diffusion cell

Chloride-induced corrosion is one of the main mechanisms of deterioration affecting the long-term performance of concrete structures (Zhang 1997). The chloride resistance depends on the permeability of the concrete and the thickness of cover to the reinforcement.

External chlorides penetrate into the interconnecting pores in concrete as bulk liquid by convection, and chloride ions diffuse further into the saturated pore system. Diffusion is controlled by concentration gradients of the free chlorides; thus the capacity of the concrete to physically adsorb and to chemically react with chloride ions affects the free chloride ions concentration in the concrete (Conciatori 2008).

The chloride resistance of concrete is thus highly dependent on the porosity of concrete in terms of pore size, pore distribution and interconnectivity of the pore system. The porosity of concrete is determined by:

- the type of cement and other mix constituents;
- concrete mix proportions;
- compaction and curing.

To prevent the chloride permeation into concrete, the use of finely grained materials (Kropp1995, Song 2008) and resin-based treatment on the cover concrete (Keer 1992) have been investigated and achieved some success.

The type of cement influences both the porosity of the concrete and its reaction with chlorides. The porosity of concrete is highly dependent on the water-cement and aggregate-cement ratios whereas the type and amount of cement affect the pore size distribution and chemical binding capacity of the concrete.

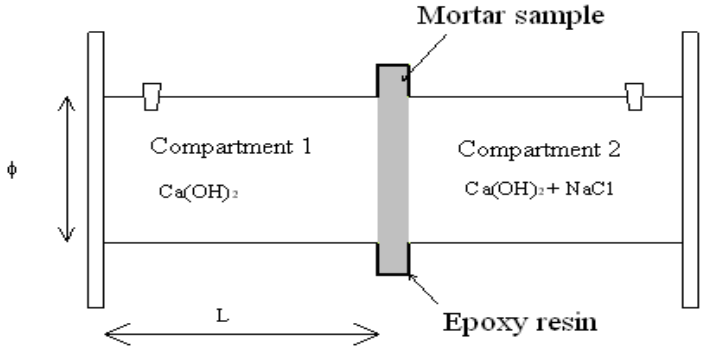

Figure V.1 *Scheme of the experimental set-up*

To discuss theoretical fundamentals of chlorides diffusion, the analysis can be referred to the same experimental set-up used to determine chloride diffusion.

Starting from the diagram of the experimental set-up used in laboratory tests and shown in Figure V.1, it is possible to distinguish three zones: the compartment 2, always maintained over time to the concentration of 3M NaCl; the specimen, through which the chloride ions diffuse from the compartment 2 to compartment 1 and the compartment 1, which undergoes the diffusive flux of chloride ions coming from the compartment 2, after diffusion through the specimen.

A typical output of this experiment is shown in Figures IV.3 and IV.4, where concentration of chlorides (in g/l), measured in the compartment 1, is plotted versus time (in days): after a lag time, the concentration of chlorides begins to grow slowly until reaching a constant value.

The domain of interest for the analysis of the problem is the compartment 1, from which the samples of solution are collected to determine the evolution of the concentrations of chloride in time. In order to know the flow of chlorides which comes from the compartment 2 to compartment 1, however, is indispensable to solve the problem of diffusion of chloride ions through the specimen, for which it is necessary to solve an equation of transport of chloride ions for pure diffusion, in accordance with the Fick's law, in transition:

$$\frac{\partial C}{\partial t} = D_{Cl\_M} \nabla^2 C \qquad \text{(V.1)}$$

where $D_{Cl\text{-}M}$ is the diffusivity of chloride ions in the mortar specimen.

From experiments, however, it is observed a long delay time in which the amount of chlorides measured in the compartment 1 is practically negligible. This suggests that, before the diffusion of chlorides occurs, the specimen must reach a certain level of water saturation.

The proposed mechanism could provides for the permeation of water (by capillarity) throughout the test specimen and then the diffusion of chlorides. This involves the addition, in the model, of an equation of permeation / diffusion of water and a condition of ON-OFF type for the diffusion of chlorides:

$$\frac{\partial C_w}{\partial t} = D_{w\_M}\nabla^2 C_w + f_e \nabla C_w \qquad \text{(V.2)}$$

where C_w is the water concentration, $D_{w\text{-}M}$ is the water diffusion in the mortar sample and f_e is the permeability factor (Guerrini 2002).

According to this scheme, only when the layers of the sample is saturated with water, the diffusion of chlorides can occur and therefore, eq. (V.1) must be solved after the solution of eq. (V.2).

Another phenomenon that must be taken into consideration is the possibility that the chlorides interact with the components present in the concrete matrix through chemical reactions or similar mechanisms analogous to chemical reactions of the type:

$$Cl^- + Y^+ \rightarrow \text{Products}$$

These phenomena could lead to the modification of eq. (V.1) as shown below:

$$\frac{\partial C}{\partial t} = D_{Cl\_w+M}\nabla C - (r_{Cl}) \qquad \text{(V.3)}$$

where D_{Cl_w+M} is the chloride diffusion in the sample satured of water and r_{Cl} represents the chloride moles reacting in the unit of time and in the unit of volume.

It 'clear that the term of consumption of the chlorides, due to a chemical interaction, disappears from the transport model when the possibility of chlorides interaction with other ions present in the concrete becomes zero due to saturation of the possible active sites.

The solution of the chloride transport equation requires an initial condition and two boundary conditions. As an initial condition, the concentration of chloride is considered null anywhere in the specimen. As boundary conditions, at the interface between the specimen and the compartment 2, is considered a 3M concentration of chloride ions and at the other interface, that between the specimen and the compartment 1, is imposed the continuity of the flow of matter.

In compartment 1, considering the fluid contained in it as static, it should be considered a diffusion equation and of possible natural convection, which

under the conditions studied is permitted neglect. The walls of the Compartments 1 and 2 (with the exception of the wall of boundary with the specimen, for which it is continuity of flow) are considered to be impermeable.

In the Compartment 1 we can write:

$$\frac{\partial C}{\partial t} = D_{Cl\_S} \nabla C \qquad \text{(V.4)}$$

where $D_{Cl\text{-}S}$ is the diffusivity of chloride ions in the solution.

The model was solved using the commercial software Comsol (release 3.4), based on FEM.

The domain of the developed model was created by assembling three primitive cylindrical representing respectively, the Compartment 1, the specimen and the Compartment 2.

Defined the transport equations for each domain, is necessary enter the equations representing the boundary conditions and values of the initial conditions.

Using the automatic procedures, the domain has been divided into finite elements, by means of the grid of the nodal points (mesh), as shown in Figure V.2. The grid in the domain representative of the specimen has been thickened, being the zone in which occurs the process object of the study.

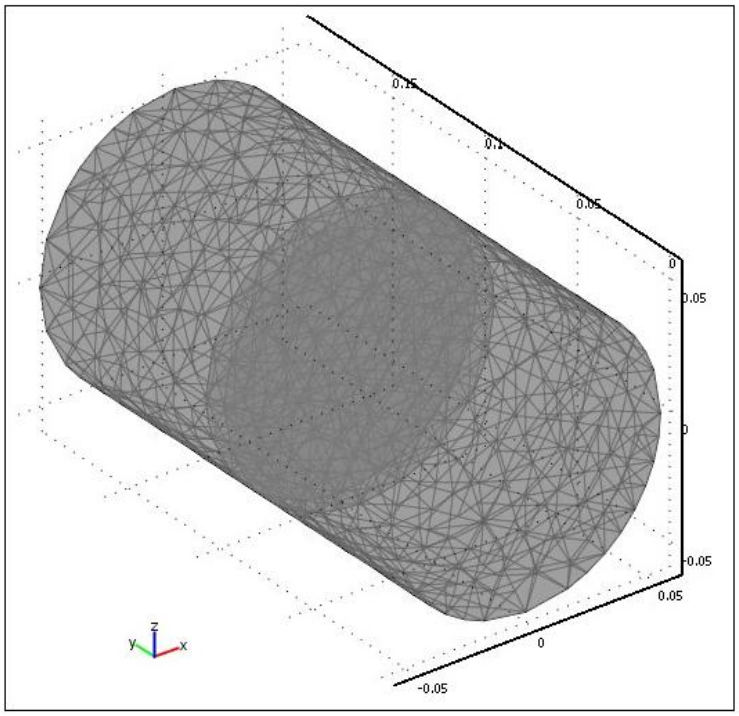

Figure V.2 G*rid of the nodal points for the implementation of the model*

The data (concentration of chloride ions in Compartment 1) were obtained by varying the diffusivity of chloride ions in the sample and comparing the numerical data with the experimental ones, leading the model to convergence through the readjustment of the value of diffusivity

The outputs can be obtained both in the form of maps of concentration, and in terms of results over time, to integrate in the entire domain of interest to obtain an average result.

In Figure V.3 is an example of output (concentration slices), in which it is possible to note how effectively the fall in concentration is realized only in the domain representative of the specimen.

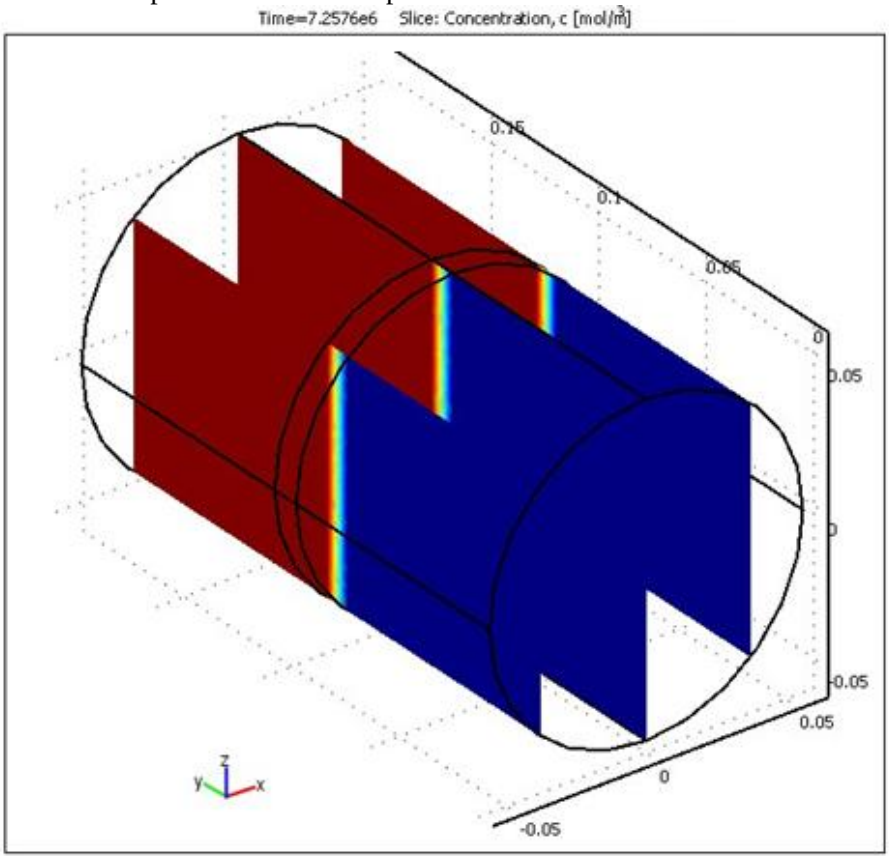

Figure V.3 *Example of model output*

The data that are obtained by the minimization of the difference between the results, in terms of concentration of chloride ions, are reported in the following Table V.1 in which is reported also the delay time of the mass transport for each sample.

Table V.1 *Experimental and theoretical diffusivity and the delay time*

Samples	Experimental Diffusivity [m^2/s]	Theoretical Diffusivity [m^2/s]	Delay Time [days]
CLS (0_0)	2,62E-12	3,55E-12	26.6
0_0.5	2,10E-12	1,85E-12	29.0
0_1	1,69E-12	2,85E-12	29.7
0_2	2,07E-12	2,50E-12	26.4
1_0	7,54E-13	2,75E-12	25.9
1_0.5	2,29E-12	2,20E-12	28.4
1_1	2,14E-12	3,30E-12	26.4
1_2	2,22E-12	No conv.	28.0

Analyzing the results, both numerical and experimental, some considerations must be done regarding the profile of the curves of accumulation of chloride in compartment 1. In fact (see Figs. IV.3 and I.V 4) all the curves show lag time that provides an idea on the time required to saturate the sample, with regard to the water content (thanks to which the chloride ions are able to diffuse) and the concrete sites in which the chloride ions can interact.

The presence of nano-clay additive and / or the use of hydrophobic resin, can change - in a more or less important way - both the lag time and the effective diffusivity. The complexity of the phenomena involved and of the chloride-structure interactions make it difficult to discuss on the effects that the added substances (nano-clay and hydrophobic agent) produce on the properties of the structure. Moreover, it should be noted that the addition of these components is made in order to modify the microporous structure of the specimens, and so it goes to affect strongly on the lag time and the effective diffusivity.

As an example, below is reported the comparison of results from experiments and from model for the cases 0_0.5 and 1_0.5 (Figure V.4). It is interesting to note that the presence of the hydrophobic resin makes the passage of the chlorides faster probably because the resin waterproofs the side walls of the pores concentrating the flow of the aqueous solution in only one direction.

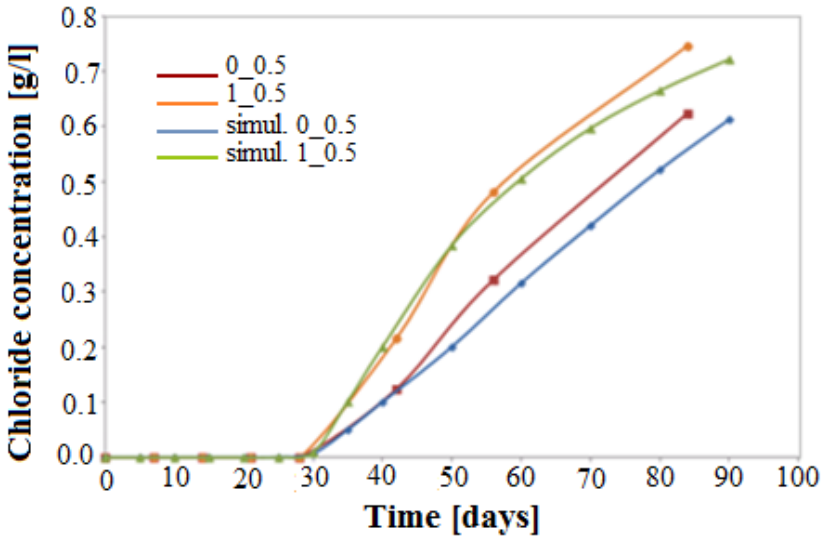

Figure V.4 *Comparison between experimental and modeling results of 0_0.5 and 1_0.5 samples*

Conclusions

During the first and second years of this Ph. D. thesis the research was pointed to the evaluation of transport properties of concrete, due to the fundamental role that transport phenomena play in the durability performances. A literature reviewing indicated that a strategy of controlling the transport properties of concrete can be represented by surface treatments.

Thus, our attention was dedicated to study the possibility of enhance the protective action of commercial polymeric based products by their modification with nanoparticles which are expected to enhance the barrier properties of the resins themselves.

Commercial polymeric treatments (Fluoline CP acting as coating and Antipluviol S acting as pore liner) were mixed with small amounts (0, 2, 4, 6 wt%) of an organomodified sodium montmorillonite (Cloisite 30B) which was dispersed on a nanoscale level by a laboratory sonication procedure. According to the reported results, it was shown that the barrier properties to water vapor were increased up to 30% in the case of nanocomposite coating resins with 6 wt% of nanoclay thus confirming the marked effect of lamellar nanoclay in reducing the permeability of polymeric resins. The positive effect of nanoclay content was also confirmed by sulphates attack resistance of concrete treated samples. Conversely, transport properties to liquid water, namely the capillary sorption coefficient, exhibit a sensible reduction related to Cloisite loading only for the coating based nanocomposite treatment.

The sorptivity coefficient is evidently reduced also in the case of concrete samples treated with Halloysite, but without any relation with the clay amount, probably this is due to the fact that the Halloysite because of its tubular morphology at high percentage is more difficult to exfoliate than the lamellar clay.

In any case, the experimental data reveal that the properties improvement due to the presence of nanoclay depend on the type of resin used as matrix.

In fact, a significant difference has been shown between the coating and pore liner based nanocomposite systems with better performance found for the latter. This behavior can be explained by considering that the pore liner can deeply penetrate into the concrete whereas the coating remains as a thin film on the surface (as confirmed by SEM micrographs). In this case a

higher incidence of clay with its hydrophilic character is obtained on the treated surface.

Although this hypothesis was in part confirmed by contact angle measurements, the results are also related to the reduction of diffusion kinetics of the polar molecules (water, sulphates) due to decreasing of the porosity of the CLS in consequence of superficial treatments, as demonstrated with mercury intrusion porosimetry.

Regarding the UV weathering of the nanocomposite films obtained by solvent casting, the results obtained in the work have shown that the nanoscale dispersion of little amounts of layered silicate particles inside polymeric surface treatments has really promising effects for conservation and protective purposes since, compared to the neat resins, nanocomposite systems can more efficacy delay the weathering phenomena of a substrate. In fact, the nanocomposites were characterized by higher thermal and photo-oxidative stability, improved hydrophobic character and negligible chromatic difference.

At the same time, as largely discussed before, a correct formulation of the mix design of concrete is fundamental to prevent the environmental attacks; thus the last part of this PhD work has been pointed to study the possibility of changing the formulation of a traditional concrete in order to make it intrinsically hydrophobic or reduce its porosity, using as hydrophobic agent a silane resin in water base and as nanoparticles two different types: one is the *Cloisite 30B* and the other one is an aluminosilicate clay nanotube, the Halloysite.

Thus, during the third year the work was aimed to investigate the separated and combined effect of both actions (hydrophobic resin and the nanoparticales at different amount) on concrete durability. In particular the results of the different tests performed lead to the following conclusions:

- The nanocomposite concrete show efficacy in inhibiting the water absorption and gas transport thanks to the reaction of the nanoclay with calcium hydroxide crystals which modify internal microstructure of mortars, making more difficult the passage of the substances. The results obtained, anyway, are almost independent on clay loading;
- Hydrophobic concrete very effectively avoids the water inlet, but because of its hydrophobic character makes the pores of concrete unsatured of water and the gas can diffuse faster through the concrete bulk.
- Finally, comparing the performances of the surface hydrophobic treatment and of the hydrophobic resin added to concrete mix to prevent the capillary suction, emerges a very important result: the resin added to concrete mix is four time more efficient respect the surface treatment in reducing the capillary adsorption.

In fact analyzing the results relative to the adsorption coefficient (CA) by capillary (see Tables III.3 and IV.1), focusing the attention on the same kind

of resin, is evident that while the pore liner resin applied as surface protective is able to reduce the water absorption ability of concrete of about 108%, the same resin added to the concrete mixing, which makes the whole concrete bulk hydrophobic, reduces the water absorption by capillary of about 413%, that is four time more.

References

Aguiar, J. B. Camoes, A. Moreira, P. M. 2008. Coatings for concrete protection against aggressive environments. *Journal of Advanced Concrete Technology* 6 (1), p. 246-250.

Aimin X, Chandra S. Influence of polymer addition on the rate of carbonation of Portland cement paste. *The International Journal of Cement Composites and Lightweight Concrete* 1988; 10 (1): 49-51.

Aldred J.M., Swaddiwudhipong S., Lee S.L., Wee T.H. The effect of initial moisture content on water transport in concrete containing a hydrophobic admixture. *Magazine of Concrete Research* 2001; 53 (2): 127–134

Almusallam A.A., Khan, F.M. Dulaijan, S.U. OAl-amoudi, .S.B. 2003. Effectiveness of surface coatings in improving concrete durability. *Cement & Concrete Composites* 25, p. 473-481

ASTM C88-05 Standard Test Method for Soundness of Aggregates by Use of Sodium Sulfate or Magnesium Sulfate, 2005.

ASTM E96-95 Standard Test Methods for Water Vapor Transmission of Materials, 1995.

ASTM C1012 / C1012M - 10 Standard Test Method for Length Change of Hydraulic-Cement Mortars Exposed to a Sulfate Solution

Basheer, L., Kropp, J., Cleland, D. J., Assessment of the durability of concrete from its permeation properties: a review. *Construction and Building Materials* 2001; (15): 93 – 103.

Cai, H., Liu, X. Freeze-thaw durability of concrete: ice formation process in pores. *Cement and Concrete Research*. 28(9), p. 1281–1287.

Conciatori, D. Sadouki, H. Brühwiler, E. 2008 Capillary suction and diffusion model for chloride ingress into concrete. *Cement and Concrete Research.* 38, p. 1401–1408

Courard L., Degeimbre R. A capillary action test for the investigation of adhesion in repair technology. *Canadian Journal of Civil Engineering* 2003; 30: 1101-1110.

Courard L., Evaluation of thermodynamic properties of concrete substrates and cement slurries modified with admixtures. *Materials and Structures* 2002; 35, p. 149-155.

D'Arienzo L., Scarfato P., Incarnato L. 2008 New polymeric nanocomposites for improving the protective and consolidatine efficiency of tuff stone. *Journal of Cultural Heritage* 9, p. 253-260.

Dulaijan, S.U., Maslehuddin, M., Al-Zahrani, M.M., Sharif, A.M., Al-Juraifani, E.A., Al-Idi, S.H. 2000 Performance evaluation of resin based surface coatings. In: *Proceeding of 6th International Conference in Deterioration and Repair of Reinforced Concrete* in the Arabian Gulf, Bahrain; p. 345-362.

Dweck, J. Ferreira da Silva, P.F. Büchler, P.M. Cartledge, F.K. 2002 Study by thermogravimetry of the evolution of ettringite phase during type II Portland cement hydration. *Journal of Thermal Analysis and Calorimetry*. 69 (1), p.179 – 186.

European Standard UNI EN 197-1 Cement - Part 1: Composition, specifications and conformity criteria for common cements, 2007.

European Standard UNI EN 772-11. Determination of water absorption of aggregate concrete, manufactured stone and natural stone masonry units due to capillary action and the initial rate of water absorption of clay masonry units, 2001.

European Standard UNI EN 13295 (2005) Products and systems for the protection and repair of concrete structures - Test methods - Determination of resistance to carbonation

European Standard UNI CEN/TS 12390-11 (2010) Testing hardened concrete - Part 11: Determination of the chloride resistance of concrete, unidirectional diffusion

Fernandez R, Martirena F, Scrivener K.L. The origin of pozzolanic activity of calcined clay minerals: A comparison between kaolinite, illite and montmorillonite. *Cement and Concrete Research* 2011; 41: 113 – 122.

Garboczi E.J. Permeability, diffusivity and micro-structural parameters. A critical review. *Cement and Concrete Research* 1990; 20: 591 – 601.

Glasser, F. P. Marchand, J. Samson, E. 2007. Durability of concrete – Degradation phenomena involving detrimental chemical reactions. *Cement and Concrete Research* 38, p. 226-246.

Guerrini, G. Borsa, M. Mensitieri, G. La diffusione degli ioni cloruro in calcestruzzi esposti ad ambiente marino temperato. Estratto dagli atti del 14° *Congresso C.T.E.* Mantova, 7-8-9 novembre 2002

He X, Shi X. Chloride permeability and microstructure of Portland cement mortars incorporating nanomaterials. *Journal of the Transportation Research Board.* 2008; 13 – 21.

Ibrahim, M., Al-Gahtani, A.S., Maslehuddin, M. 1999 Use of surface treatments materials to improve concrete durability. *ACI Mater J.* II(1) p. 36-40.

Italian Recommendation NORMAL 43/93. Misure colorimetriche di superfici opache, 1993.

Italian Standard UNI 7699 (2005) Prova sul calcestruzzo indurito - Determinazione dell'assorbimento di acqua alla pressione atmosferica.

Italian Standard UNI 11164 (2005) Calcestruzzo - Determinazione della permeabilità all'ossigeno.

Ji T. Preliminary study on the water permeability and microstructure of concrete incorporating nano-SiO2. *Cement and Concrete Research* 2005; 35: 1943 - 1947.

Keer JG. Surface treatments. In: Mays G, editor. Durability of concrete structures, E&FN SPON; 1992. p. 146–65.

Kropp J, Hilsdorf HK Performance criteria for concrete durability, E&FN SPON; 1995. p. 138–64.

Kuo W-Y, Huang J-S, Lin C-H. Effect of organo-modified montmorillonite on strengths and permeability of cement mortars. *Cement and Concrete Research* 2006; 36: 886 - 895.

Leung, C. K.Y. Zhu, H. Kim, J.K. Woo, R.S.C. 2008 Use of polymer/organoclay nanocomposite surface treatment as water/ion barrier for concrete. *Journal of materials in civil engineering* 20, p. 484-492.

Li Z, Wang H, He S, Lu Y, Wang M. Investigations on the preparation and mechanical properties of the nano-alumina reinforced cement composite. *Materials Letters* 2006; 60(3):356 – 359.

Marwa M. H., Heather D., Louay N. M., Tyson R. Evaluation of the durability of titanium dioxide photocatalyst coating for concrete pavement. *Construction and Building Materials* 2010; 24 (8): 1456-1461

Medeiros, M.H.F. and Helene, P. 2009. Surface treatment of reinforced concrete in marine environment: Influence on chloride diffusion coefficient and capillary water absorption. *Construction and Building Materials* 23, p. 1476–1484.

Musso, S. Tulliani, J.-M. Ferro, G. Tagliaferro, A. 2009 Influence of carbon nanotubes structure on the mechanical behavior of cement composites. *Composites Science and Technology*. 69, p. 1985–1990

Papadakis, V. G., Vayenas, C. G., Fardis M.N. 1991 Physical and Chemical Characteristics Affecting the Durability of Concrete *Materials Journal* 88(2).

Park, D.C. 2008 Carbonation of concrete in relation to CO_2 permeability and degradation of coatings *Construction and Building Materials*. 22, p. 2260–2268.

Poon, C.S., Kou, S.C., Lam, L., Compressive strength, chloride diffusivity and pore structure of high performance metakaolin and silica fume concrete. 2006 *Construction and Building Materials* 20, p. 858–865.

Qixian, L., Bungey, J. H. Using compression wave ultrasonic transducers to measure the velocity of surface waves and hence determine dynamic modulus of elasticity for concrete. *Construction and Building Materials* 1996. 10 (4): 237–242.

Sanchez F, Sobolev K. Nanotechnology in concrete – A review. C*onstruction and Building Materials* 2010. 24: 2060-2071.

Sergi, G., Lattery, S.E., Page, C.L. Influence of surface treatments on corrosion rates of steel in carbonated concrete. *Corrosion and*

Reinforcement in Concrete 1990. London: Elsevier Applied Science; p. 409-419.

Selvaraj, R., Selvaraj, M., Iyer, S.V.K. Studies on the evaluation of the performance of organic coatings used for the prevention of corrosion of steel rebars in concrete structures. *Progress in Organic Coatings* 2009. 64, p. 454–459.

Shebl S. S., Allie L., Morsy M. S., Aglan H. A. Mechanical behavior of activated nano silicate filled cement binders. Journal of Materials Science 2009; 44:1600–1606.

Song, H.W, Kwon, S.J. Permeability characteristics of carbonated concrete considering capillary pore structure. *Cement and Concrete Research* 2007. 37, p. 909–915.

Song, H.W. Lee, C.-H. Ann, K.Y. Factors influencing chloride transport in concrete structures exposed to marine environments. *Cement & Concrete Composites* 30 (2008) 113–121.

Subramaniam, K.V, Lee J, Christensen B. J. Monitoring the setting behavior of cementitious materials using one-sided ultrasonic measurements. *Cement and Concrete Research* 2005; 35 (5): 850-857.

Tittarelli F, Moriconi G. The effect of silane-based hydrophobic admixture on corrosion of galvanized reinforcing steel in concrete. *Corrosion Science* 2010; 52: 2958–2963.

Tittarelli F, Oxygen diffusion through hydrophobic cement-based materials. *Cement and Concrete Research* 2009; 39 p. 924–928.

Vacchiano, C. D. Incarnato, L. Scarfato, P. Acierno, D. Conservation of tuff-stone with polymeric resins. *Construction and Buildings Materials* 2008. 22, p. 855-865.

Vipulanandan, C., Liu, J. Performance of polyurethane-coated concrete in sewer environment. *Cement and Concrete Research* 2005. 35, p. 1754–1763.

Woo, R.S.C. Zhu, H. Chow, M.M.K. Leung, C. K.Y. Kim, J.K. Barrier performance of silane-clay nanocomposite coatings on concrete structure. *Composites Science and Technology* 2008. 68, p. 2828-2836.

Woo, R.S.C., Chen, Y., Zhu,H., Li, J., Kim, J.K., Leung, C. K.Y. 2007 Environmental degradation of epoxy–organoclay nanocomposites due to

UV exposure. Part I: Photo-degradation. *Composites Science and Technology*. 67, p. 3448-3456.

Woo, R.S.C., Chen, Y., Zhu,H., Li, J., Kim, J.K., Leung, C. K.Y. 2008. Environmental degradation of epoxy-organoclay nanocomposites due to UV exposure: Part II residual mechanical properties. *Composites Science and Technology*. 68, p. 2149 –2155.

Wright W.M.D. Analytical Methods | Ultrasonic Techniques. *Encyclopedia of Dairy Sciences (Second Edition)* University College Cork, Cork, Ireland, 2011, p. 206 - 214.

Ye, Q. Zhang, Z. Kong, D., Chen, R. 2007 Influence of nano-SiO2 addition on properties of hardened cement paste as compared with silica fume. *Construction and Building Materials.* 21, p. 539 – 545.

Zelic, J. Rusic, D. Veza, D. Krstulovic, R. (2000) The role of silica fume in the kinetics and mechanisms during the early stage of cement hydration. *Cement and Concrete Research.* 30, p. 1655–1662.

Żenkiewicz M.. Methods for the calculation of surface free energy of solids. *Journal of Achievements in Materials and Manufacturing Engineering* 2007. 24(1), p. 137-145.

Zhang, J. -Z. McLoughlin, I. M. Buenfeld, N. R. 1997. Modelling of chloride diffusion into surface-treated concrete. *Cement and Concrete Composites.* 20, p. 253 – 261.